Virus Research 350 (2024) 199476

Contents lists available at ScienceDirect

Virus Research

journal homepage: www.elsevier.com/locate/virusres

Dothistroma septosporum and *Dothistroma pini*, the causal agents of Dothistroma needle blight, are infected by multiple viruses

Miloš Trifković [a,*], Ondřej Hejna [b], Anna Kuznetsova [a], Martin Mullett [a], Libor Jankovský [a], Leticia Botella [a]

[a] Department of Forest Protection and Wildlife Management, Faculty of Forestry and Wood Technology, Mendel University in Brno, Czech Republic
[b] Department of Genetics and Agricultural Biotechnology. Faculty of Agriculture and Technology, University of South Bohemia in České Budějovice, Czech Republic

ARTICLE INFO

Keywords:
Dothistroma needle blight (DNB)
Conifer pathogens
Virus diversity
Total RNA sequencing
High-throughput sequencing

ABSTRACT

Dothistroma septosporum and *Dothistroma pini* are severe foliar pathogens of conifers. They infect a broad spectrum of hosts (mainly *Pinus* spp.), causing chlorosis, defoliation of needles, and eventually the death of pine trees in extreme cases. Mycoviruses represent a novel and innovative avenue for controlling pathogens. To search for possible viruses hosted by *Dothistroma* spp. we screened a subset of isolates (20 strains of *D. septosporum* and one *D. pini*) originating from the Czech Republic, Slovenia, Italy, Austria and Ireland for viral dsRNA segments. Only five of them showed the presence of dsRNA segments. A total of 21 fungal isolates were prepared for total RNA extractions. RNA samples were pooled, and two separate RNA libraries were constructed for stranded total RNA sequencing. RNA-Seq data processing, pairwise sequence comparisons (PASC) and phylogenetic analyses revealed the presence of thirteen novel putative viruses with varying genome types: seven negative-sense single-stranded RNA viruses, including six bunya-like viruses and one new member of the order *Mononegavirales*; three positive-sense single-stranded RNA viruses, two of which are similar to those of the family *Narnaviridae*, while the genome of the third correspond to those of the family *Gammaflexiviridae;* and three double-stranded RNA viruses, comprising two novel members of the family *Chrysoviridae* and a potentially new species of gammapartitivirus. The results were confirmed with RT-PCR screening that the fungal pathogens hosted all the viruses and showed that particular fungal strains harbour multiple virus infections and that they are transmitted vertically. In this study, we described the narnavirus infecting *D. pini*. To our knowledge, this is the first virus discovered in *D. pini*.

1. Introduction

Dothistroma needle blight (DNB), formerly known as red-band needle blight, is one of the most important foliar diseases of members of the *Pinaceae* family, affecting over 110 species, mainly *Pinus* spp. (Drenkhan et al., 2016; van der Nest et al., 2023). DNB is caused by two closely related fungal species, *Dothistroma septosporum* (Doroguine) Morelet and *D. pini* Hulbury (Barnes et al., 2004, 2016). The former is most likely of Eurasian origin and currently has a worldwide distribution (Mullett et al., 2021). Contrarily, its sister species, *D. pini*, has a more limited distribution and has been reported only in the USA and Europe (van der Nest et al., 2023). Both fungi cause similar symptoms, initiated as chlorosis progressing to necrosis of the distal part of the needle. A typical symptom is the appearance of red discolouration around the necrotic spots due to the accumulation of dothistromin, a toxin produced by the fungus (Bradshaw, 2004). The disease culminates as a needle cast, which may induce tree death in extreme cases (Barnes et al., 2004; EPPO, 2015). Total losses due to DNB, only in the UK, including wood and non-wood damages, are estimated to be in tens of millions of GBP annually (for details, see Mullett et al., 2021). Given its importance, many different approaches to controlling and managing DNB have been suggested (Bulman et al., 2016). More recently, the potential of spraying ultra-low volume aerial fungicides to control outbreaks of DNB in the UK has been highlighted (Tubby and Forster, 2021). However, given the EU's strict regulations over pesticide usage in plantations and natural forests, there is urgent need for more environmentally friendly tools against tree pathogens. Employing mycoviruses, that reduce virulence of plant pathogen (hypovirulence), as biological control agents (BCAs) could be an attractive alternative against fungal pathogens (García-Pedrajas et al., 2019; Muñoz-Adalia et al., 2016; Prospero et al.,

* Corresponding author.
E-mail address: milos.trifkovic@mendelu.cz (M. Trifković).

https://doi.org/10.1016/j.virusres.2024.199476
Received 19 June 2024; Received in revised form 22 September 2024; Accepted 27 September 2024
Available online 5 October 2024

2021).

Over 60 years have passed since the first discovery of mycoviruses infecting the cultivated mushroom *Agaricus bisporus* (Hollings, 1962). It is now established that fungi are commonly subjected to viral infections (Ghabrial et al., 2015). Over the past decade, the decreasing costs of high-throughput sequencing (HTS) services and advances in metagenomics have shed light on a hidden universe of enormous viral diversity infecting different organisms, including fungi (Zhang et al., 2019). Mycoviruses are sorted into 23 families containing over 200 species, with plenty more awaiting assignment to existing or new families by the International Committee on Taxonomy of Viruses (ICTV) (Kondo et al., 2022). As they lack an extracellular phase, mycoviruses need cell-to-cell contacts for transmission. In nature, they are transferred horizontally via anastomosis between vegetatively compatible hyphae or vertically by spores, where transmission via conidia (asexually produced spores) is more often than via ascospores (sexually produced spores) (Ghabrial and Suzuki, 2009; Pearson et al., 2009).

Forest pathologists have strived for many years to replicate the success of controlling *Cryphonectria parasitica* with the mycovirus Cryphonectria hypovirus 1 (Anagnostakis, 1982; Heiniger and Rigling, 1994). Guided by the same principle, many important conifer pathogens have been tested for mycoviruses. One of the first to be investigated was the globally distributed latent pine pathogen *Diplodia sapinea* (Fr.) Fuckel (syn. *Sphaeropsis sapinea* (Desm.) Kickx.), in which researchers from South Africa described two totiviruses, named Sphaeropsis sapinea RNA virus 1 and 2 (SsRV1 and SsRV2) (Preisig et al., 1998). Viruses belonging to the families *Mitoviridae* and *Totiviridae* have been discoverd infecting the rust fungus *Cronartium ribicola* (J.C. Fisch) (Liu et al., 2019, 2016). In *Gremmeniella abietina* var. *abietina* (Lagerb.) Morelet biotype A, the causative agent of Scleroderris canker, a totivirus closely related to SsRV2, has been reported (Tuomivirta and Hantula, 2003a). The same biotype has been found to be infected by partitiviruses, totiviruses and mitoviruses (Botella et al., 2012, 2015b; Botella and Hantula, 2018; Tuomivirta and Hantula, 2003b, 2003a, 2005), while *G. abietina* biotype B is a host to an endornavirus (Tuomivirta et al., 2009). *Fusarium circinatum* Nirenberg & O'Donnell, the cause of the severe conifer disease, pine pitch canker, also harbours members of the family *Mitoviridae* (Martínez-Álvarez et al., 2014; Muñoz-Adalia et al., 2018; Vainio et al., 2015b). Wood-decay fungi from the *Armillaria* genus are infamous pathogens of many important conifers. Linnakoski et al. (2021) characterized one mycovirgavirus and three ambi-like viruses in *A. borealis* Marxm. & Korhonen, two of each mymona-like, ourmia-like and ambi-like viruses in *A. mellea* (Vahl) P. Kumm isolates. In the same study, three distinctive ambi-like viruses were found infecting *A. ectypa* (Fr.) Lamoure, *A. luteobubalina* Watling & Kile and *A. novea-zelandiae* (G. Stev.) Boesew., respectively. Additionally, the ambi-like virus was reported in the Czech population of *A. ostoyae* (Romagn.) Herink (Tonka et al., 2022).

The most explored conifer pathogen's virome is hosted by *Heterobasidion* spp., causing root and stem rot in conifers and has been summarised by Hantula et al. (2020), Vainio (2019) and Vainio and Hantula (2016). Following their screening, two particularly promising mycoviruses, namely HetPV13 and HetPV15, were identified for their synergic efficacy in disrupting the mycelial growth of *Heterobasidion parviporum* (Kashif et al., 2019; Vainio et al., 2018b). The exploration of mycoviruses becomes essential due to the high potential for their application as biocontrols against significant plant pathogens. The first mycovirus was recently described from *D. septosporum* when the complete sequence of an alphachrysovirus was reported (Daudu et al., 2019; Shah et al., 2023).

Due to these reasons, we aim to screen a collection of *Dothistroma* spp. isolates for mycoviruses using classical double-stranded (ds) RNA purification and total RNA sequencing. The specific objectives were to (i) discover and characterize novel viruses and (ii) assess the virus's vertical transmission rate through fungal conidia.

2. Materials and methods

2.1. Fungal isolates

Twenty isolates of *D. septosporum* and one isolate of *D. pini* were used. Pine needle samples with typical symptoms of DNB were collected in May and June 2019 in the Czech Republic, Slovenia and Italy. The fungus was isolated using the acervuli rolling technique, detailed in Mullett and Barnes (2012). An additional six *D. septosporum* isolates from the Czech Republic, one isolate from Austria, and a single *D. pini* isolate from the Czech Republic were added. These isolates were sourced from the fungal culture collection at the Department of Forest Protection and Wildlife Management at Mendel University in Brno. Two Irish isolates from Mullett et al. (2018) were also included. For more information about fungal strains, see Supplementary Table S1.

All fungal isolates were identified to the species level by using i) morphological features (as described by Barnes et al. (2004) and Mullett and Barnes (2012)), ii) sequencing the internal transcribed spacer (ITS) region of rDNA using primer pair ITS5 and ITS4 (White et al., 1990). The identity of the species was confirmed by aligning the sequences to the reference sequences using NCBI BLAST (Altschul et al., 1990; Sayers et al., 2023). The fungal strains were maintained on potato dextrose agar (PDA; HiMedia Laboratories Pvt. Ltd. Mumbai, India). For dsRNA and total RNA extractions, isolates were grown on PDA (HiMedia) covered with a cellophane sheet (EJA08–100, Gel Company Inc., San Francisco, CA, United States).

2.2. dsRNA extractions

To screen the presence of dsRNA segments, highly indicative of virus presence, in our *Dothistroma* spp. isolate collection, we used the protocol of Morris and Dodds (1979), adapted and described by Tuomivirta et al. (2002). For each *Dothistroma* spp. isolate, approximately 2 g of fresh mycelium was harvested after being grown on PDA with cellophane for two weeks. The mycelium was collected in a 50 ml Falcon tube with four or five 6.35 mm (1/4 inch) ceramic spheres (M.P. Biomedicals, LLC, Solon, OH, United States) and immersed into liquid nitrogen. The homogenization of fungal material was done by vortexing using the Vortex-Genie 2 (SI-0256; Scientific Industries, Inc., Bohemia, NY, United States). DsRNA bands were visualized in 1–1.2 % agarose gels stained with SERVA DNA Stain G (SERVA Electrophoresis GmbH, Heidelberg, Germany) under UV light.

2.3. Total RNA extractions

Approximately 100 mg of fresh mycelium were harvested into micro tubes containing glass beads and immediately dunked into liquid nitrogen. For total RNA extractions, RNAzol® RT (Sigma-Aldrich GmbH, Steinheim, Germany) was used following the protocol described by Chomczynski et al. (2010), with a slightly modified homogenisation step. Briefly, the homogenisation of the mycelium was done on a Mixer Mill MM 400 (Retsch GmbH, Haan, Germany) at 30 Hz using the following setup: twice for 30 s flash-freezing the samples in liquid nitrogen between steps, and once for 1 min with the mycelia samples immersed in RNAzol® RT (Sigma-Aldrich). Total RNA quality was estimated by visualisation on an agarose gel under UV light, quantified using a Qubit® 2.0 Fluorometer (Life Technologies, Thermo Fisher Scientific), and stored at -80 °C.

2.4. Stranded total RNA sequencing

An equal volume of total RNA from 21 *Dothistroma* spp. isolates were pooled according to the provenances of the fungal material (Supplementary Table S1). Two RNA pools of *Dothistroma* spp. (11 samples in pool 1 (do1) and 10 in pool 2 (do2)) were sent for library preparations and sequencing to the Institute of Applied Biotechnologies Inc. (Prague,

Czechia). RNA quantity and quality were assessed with a Qubit® 2.0 Fluorometer (Life Technologies, Thermo Fisher Scientific) and a 2100 Bioanalyzer (Agilent Technologies). Approximately 1 μg of total RNA free of genomic DNA was depleted of rRNA using the NEBNext rRNA Depletion Kit (Human/Mouse/Rat). All libraries were constructed with the NEBNext Ultra II Directional RNA Library prep kit and NEBNext Multiplex Oligos for Illumina (Unique Dual Index Primer Pairs) (NEB, Ipswich, MA, USA) and sequenced on a NovaSeq 6000 (Illumina) for pair-end (2 × 150 nt) sequencing on a NovaSeq6000 (DS-150) (Illumina, San Diego, CA, USA) using a NovaSeq S4 v1.5 reagent kit. An "in-lane" PhiX control was included in each flow cell lane.

The raw reads are available at the NCBI Sequence Read Archive (SRA) as the BioProject ID PRJNA913395 and BioSample IDs SAMN26499397 and SAMN26499398.

2.5. Virus assembly and detection -in silico analyses

Bcl2fastq v2.20.0.422 Conversion Software (Illumina) automatically processed the generated data, which performed base-calling, basic adapter clipping, and quality filtering. The raw data was downloaded from the BaseSpace cloud servers (Illumina) and processed on a local server. The first step covered the data quality check using the FastQC v0.11.9 program available at https://www.bioinformatics.babraham.ac.uk/projects/fastqc/. Due to the partial presence of adapter sequences and the insufficient quality of the sequencing data, adapter and quality trimming were performed. The correctness of adapter sequences was verified in the BBTools v37.87 software package (Bushnell et al., 2017) available at https://jgi.doe.gov/data-and-tools/software-tools/bbtools/. The quality (phred score 30+, length 50+ bp) and adapter trimming were done with Trimmomatic v0.39 (Bolger et al., 2014), available at http://www.usadellab.org/cms/?page=trimmomatic. Subsequently, the output data quality was again evaluated using the FastQC.

Due to previous experience with high ribosomal (r) RNA content in the sequencing data, the program SortMeRNA v4.3.6 (Kopylova et al., 2012), available at https://github.com/sortmerna/sortmerna, was used to remove host-derived rRNA. The source rRNA sequences were obtained from the SILVA database at https://www.arb-silva.de/, and the GenBank assembly GCA_002236755.2 containing the genome sequence and an annotation GTF file with the position of the genes of *D. septosporum* was used as a reference sequence. The alignment was performed by the STAR v2.7.9a program (Dobin et al., 2013). All mapped reads were removed from further analyses.

To verify the presence of already published viruses, an alignment was performed to all complete viral refseq sequences from the NCBI database available at https://www.ncbi.nlm.nih.gov/labs/virus/vssi/#/ (accessed date: 3/24/2023). The alignment was performed with the BWA v0.7.17.-r1188 program package (Li and Durbin, 2009), which is available at https://bio-bwa.sourceforge.net/. The coverage was calculated for each reference sequence using SAMtools v1.16.1 (Li et al., 2009), available at https://github.com/samtools/samtools. For sequences with coverage higher than 80 %, the alignment was visualized using the software IGV v2.16.1 (Robinson et al., 2011), available at https://software.broadinstitute.org/software/igv/.

Unmapped reads generated by STAR were used for *de novo* assembly. The program SPAdes v3.15.5 (Bankevich et al., 2012), with default settings for metagenomics, was used as an assembler (available at https://github.com/ablab/spades). Contigs assembled by SPAdes were filtered in three steps. In the first step, all contigs smaller than 500 bp were removed. In the next step, the remaining contigs were tested by ORFfinder v0.4.3 (Rombel et al., 2002) for open reading frames (ORF). The program is available online and locally at https://www.ncbi.nlm.nih.gov/orffinder/. If no ORFs were detected in the contig, it was discarded. The last filtering step was the calculation of the average coverage. Reads after rRNA removal using BWA were mapped to contigs with detected ORFs. Subsequently, the average coverage for the contigs was calculated using the samtools program. The contig was deleted if the average coverage did not reach depth 5.

The whole RefSeq non-redundant protein (nr) database from NCBI, available at https://www.ncbi.nlm.nih.gov/refseq/about/non-redundantproteins/, was downloaded to a local server on 24/3/2023. The DIAMOND v2.0.15 program (Buchfink et al., 2015) was used to search for similarities between the nr database and the remaining contigs. The search was sped up by being divided into three phases. In the first phase, contigs were tested against the nr database with virus taxid specified and the e-value threshold was set to $1e^{-3}$. If at least one hit was reached, the contig was used to search for similarity to the nr database with the dothistroma taxid specified. In the last phase, contigs were tested against the whole nr database.

2.6. Sequence analyses, genetic variability, and phylogenetic trees

Analyses of assembled putative viral nucleotide sequences were executed using the bioinformatics software Unipro UGENE 49.0 (Okonechnikov et al., 2012). The software was used to detect ORFs, protein translations, pairwise sequence comparison (PASC) and determine the number of reads. To estimate the depth of coverage, we used the following formula:

$$\frac{\textit{total reads mapped to the final virus sequence} \times \textit{average read length}}{\textit{virus genome or contig length}}$$

After aligning the viral nucleotide and protein sequences with MUSCLE (Edgar, 2004), the pairwise identities were calculated and presented as similarity percentages (Supplementary Tables S6-S20). Deduced amino acids (aa) sequences of all genomic segments of new putative viruses were aligned to aa sequences of related viruses from GenBank using MUSCLE (Edgar, 2004) under Unipro UGENE 49.0 (Okonechnikov et al., 2012) to inspect possible conserved motifs in proteins. Furthermore, the NCBI CD-search tool (https://www.ncbi.nlm.nih.gov/Structure/cdd/wrpsb.cgi), which was last accessed on 08/09/2023, was utilized to identify potential conserved domains.

Phylogenetic analyses were performed in RAxML-HPC v.8 on XSEDE conducted in the CIPRES Science Gateway (Miller et al., 2010). To assign viruses to families and genera, phylogenetic trees were constructed using the maximum likelihood (ML) method (Stamatakis et al., 2008). The GAMMA model was used to prevent thorough optimization of the best-scoring ML tree at the end of the run. The Jones-Taylor-Thornton (JTT) model was used as a protein substitution model. Branch support was calculated using bootstrapping with parameters the CIPRES Science Gateway recommended. FigTree 1.4.4. (http://tree.bio.ed.ac.uk/software/figtree/) was used for visualisation of the phylogenetic trees.

2.7. RT-PCR confirmation and detection of mycoviruses in Dothistroma spp. isolates

We used RT-PCR with virus-specific primers (Supplementary Table S2) to confirm the individual hosts of the new putative mycoviruses. The specific primers were designed in Primer 3 under Geneious Prime® 2020.2.3 to amplify fragments of all viral genomic segments assembled *in silico*. DNA copies of the original total RNA were synthesised using the High-Capacity cDNA Reverse Transcription Kit (Applied Biosciences, Park Ave, NY, United States) following the manufacturer's recommendations with the denaturation of RNAs for 10 min at 65 °C. PCRs were performed with 12.5 μl 2X Phire Green Hot Start II PCR Master Mix (F126S, Thermo Scientific®, Thermo Fisher Scientific), 1 μl of each 10 mM primer, 3 μl of cDNA and adding PCR grade water up to a final volume of 25 μl. Cycling conditions were set according to the manufacturer's instructions with an annealing temperature of 60 °C for all primers. PCR products were visualised with ultraviolet trans-illumination in 1–1.2 % agarose gels, and amplicons of the correct expected size were sent to Eurofins Genomics (Ebersberg, Germany) for Sanger sequencing.

2.8. Bunyavirus vertical transmission via conidia

In order to assess the vertical transmission of a virus-infected isolate of *D. septosporum*, we generated 96 monosporic cultures of the *D. septosporum* isolate 1343. The RT-PCR showed that isolate 1343 was infected by only one bunyavirus, with the proposed name Dothistroma septosporum bunya-like virus 1 (DsBLV1) (see results). To induce sporulation in vitro, we plated the 1343 isolate on PDA (HiMedia) and Dothistroma Sporulating Medium (DSM), as described in Mullett and Barnes (2012). The Petri plates were incubated in the dark at 16 °C. After 4 to 5 weeks, the formation of conidia was observed. The presence of conidia was also confirmed using the Olympus BX50 polarised light microscope. Conidia were washed off mycelium with sterilised water, and spore suspension was pipetted onto a plate with PDA. After 2 or 3 days, the germinating monoconidial hyphae were transferred to clean media using a sterile needle under the stereomicroscope. Monosporic isolates needed at least four weeks to grow enough mycelium for further analyses. Total RNA extractions and cDNA synthesis were done as described above. RT-PCR with virus-specific primers was used to confirm the presence of all three genome segments of DsBLV1.

3. Results and discussion

3.1. dsRNA screening

A total of 26 isolates of *D. septosporum* and one isolate of *D. pini* collected from symptomatic *Pinus* spp. in different localities in Central Europe and Ireland (Supplementary Table S1) were screened for the presence of viruses. Five (19.23 %) isolates of *D. septosporum* revealed two different dsRNA banding patterns on the agarose gel (Fig. 1D). Two isolates from the Czech Republic contained dsRNA binding profiles resembling the *Chrysoviridae* family viruses (4 dsRNA fragments between ca. 3–4 kb). The dsRNA binding pattern of two Italian isolates resembled those of the *Partitiviridae* family (one dsRNA fragment of ca. 2 kb and the other closer to 1.5 kb). One isolate from Slovenia (PIŠ3.16) contained both dsRNA-above-mentioned profiles. No putative dsRNA banding patterns belonging to the ssRNA viruses found in this study by HTS appeared visible in the gel. This agrees with other studies where ssRNAs were not detected for (+)ssRNA viruses uncovered by HTS (Linnakoski et al., 2021). Generally, (+)ssRNA genomes often have low copy numbers of replicative dsRNA form (Vainio et al., 2015a). In the case of bunyaviruses and other (-)ssRNA viruses, their genome replication strategy prevents the possibility of visualising them by dsRNA extraction since they require the complexation of genomic and anti-genomic RNA during synthesis with viral nucleoproteins (Weber et al., 2006). It has been observed that this process effectively prevents the formation of extended dsRNA segments by inhibiting the complementary base pairing between genomic and anti-genomic RNA molecules (O'Brien et al., 2015). This enables the virus to evade the induction of cellular antiviral reactions, such as RNA interference (RNAi) and interferon signalling, for which dsRNA serves as an efficient activator (Mueller et al., 2010; O'Brien et al., 2015; Wang et al., 2016).

3.2. HTS and metatranscriptomic identification of virus-like contigs

The total number of sequenced reads in library 1 (do1) was over 700 M reads (7.6e+08) for each direction (R1 and R2) and just under 500 M (4.94e+08) in the second library (do2). After trimming and removing low-quality, host genome-mapped, low cover depth, rRNA reads, etc., the number of all assembled contigs by SPAdes was 66,083 and 35,312 in libraries do1 and do2, respectively. Detailed information about the sequencing results can be found in Supplementary Tables S3-S5. The

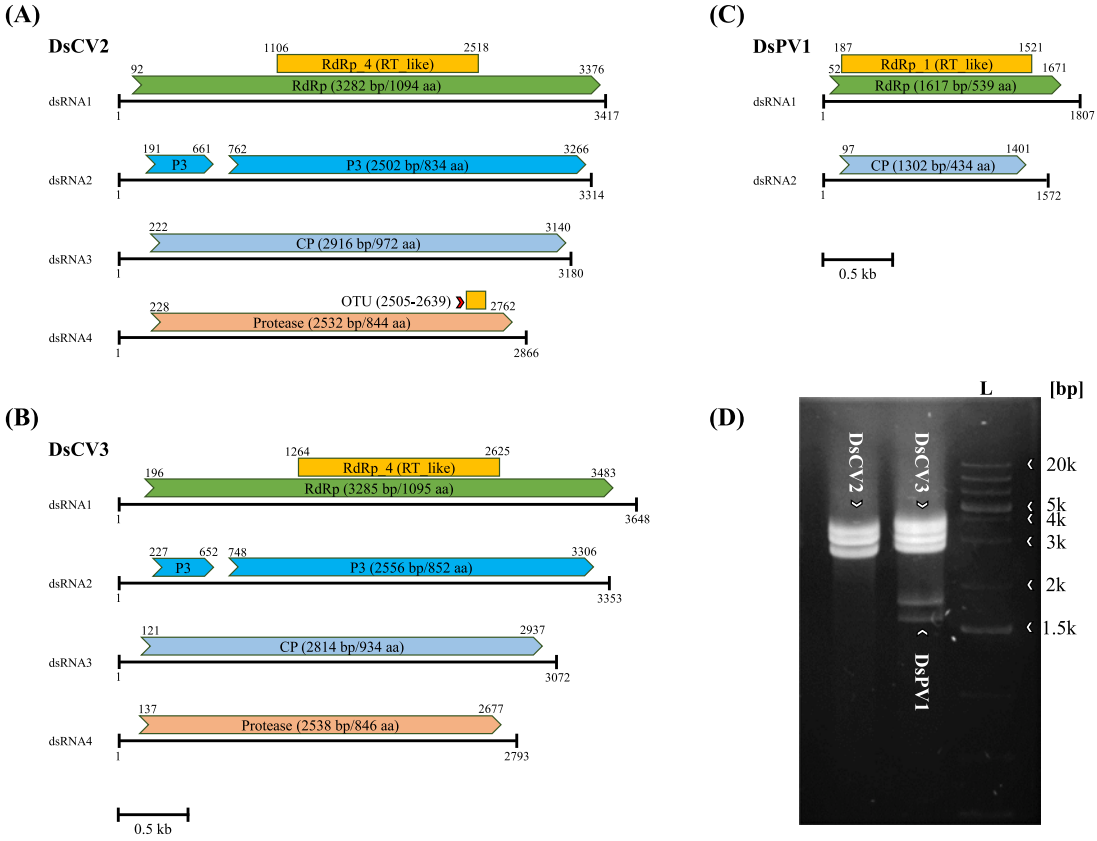

Fig. 1. Schematic representation of the genome organisation of putative dsRNA viruses from the current study with key nucleotide and amino acids specified: (A) DsCV2, (B) DsCV3 and (C) DsPV1. ORFs are presented as arrows, while rectangular yellow boxes represent conserved domains. (D) Electrophoretic banding patterns of the dsRNA elements present in *Dothistroma septosporum* isolates ŠUM 1.1.a. (left lane) and PIŠ 3.16. (middle lane). Lane L contained a genomic size marker.

difference of over 200 M reads obtained from the library do1 and do2 did not impact the coverage depth of the final virus sequences. This result suggests that the sequencing capacity requested (500–700 M reads) for a pool of 10–15 RNAs was enough for an appropriate detection and characterisation of viruses in our collection of isolates of *Dothistroma* spp.

3.3. Genome organisation of putative new mycoviruses

A total of 33 virus-like contigs scattered in both pooled RNA samples were identified. Subsequent BLASTx search associated these contigs to 13 new putative RNA mycoviruses (Table 1), including three dsRNA viruses (two chrysoviruses and one partitivirus), seven (-)ssRNA viruses (six bunya-like viruses and one mymonavirus) and three (+)ssRNA viruses (one gammaflexivirus and two narnaviruses).

3.3.1. dsRNA viruses

Not long ago, the family *Partitiviridae* was home to both partitiviruses and chrysoviruses. In 2005, in their eighth report, ICTV assigned chrysoviruses to their own family, *Chrysoviridae*, due to their increased number of genome segments and other distinguishing characteristics (Nibert et al., 2014). Today, the family *Chrysoviridae* hosts isometric, non-enveloped viruses, which possess a segmented, linear dsRNA genome consisting of three to seven segments, each individually encapsidated. It has been suggested that chrysoviruses may be responsible for the induction of hypovirulence in their fungal hosts and are known to infect fungi, plants, and potentially insects (Kotta-Loizou et al., 2020). Partitiviruses are small, isometric, and non-enveloped, with bipartite dsRNA genome, about 3–4.8 kb in size. Viruses belonging to the taxonomic family *Partitiviridae* are capable of infecting plants (predominantly angiosperms), fungi (ascomycetes and basidiomycetes), and protozoa (*Cryptosporidium* spp.) (Vainio et al., 2018a).

Two Czech isolates of *D. septosporum*, found on the same pine tree, were infected with the tetra-segmented chrysovirus, named Dothistroma septosporum chrysovirus 2 (DsCV2). The genome organisation of DsCV2 is shown in Fig. 1A. Numbers 1 to 4 were assigned to the dsRNAs according to their decreasing size. The sequence of dsRNA1 is 3417 base pairs (bp) in length (GC content 45.48 %) and contains a large single ORF that encodes a 1094 amino acid (aa) protein (126.60 kDa). NCBI CDD search found from 1106 to 2518 bp, a conserved domain belonging to pfam02123 (RdRp_4; E-value 1.66e-66), a member of the reverse-transcriptase-like superfamily cl02808. BLASTx searches indicated that dsRNA1 encoded protein shows a high degree of identity to the RNA-dependent RNA polymerases (RdRp) of members of the *Chrysoviridae* family (the highest identity was to Dothistroma septosporum virus 1 (DsCV1) RdRp, with 72.26 % identity). Sequence analysis of dsRNA2 revealed that it is 3314 bp long and contains two ORFs encoding 156 and 834 aa proteins (19.07 kDa and 94.59 kDa), P3S and P3, respectively. BLASTp search of the P3S found no significant similarity in the database. A later BLASTx search of the larger dsRNA2 protein showed high identity to hypothetical proteins (HP) of different members of the family *Chrysoviridae*, with DsCV1 HP being the most closely related (48.47 % identity). dsRNA3 is 3180 bp long and contains a single ORF that encodes a 972 aa protein (107.53 kDa). BLASTx searches of the sequence of dsRNA3 showed the highest identity with a capsid protein (CP) of DsCV1 (53.62 % identity). dsRNA4 is 2866 bp in size with a single ORF that encodes an 844 aa protein (93.62 kDa). The analysis of the protein coded by dsRNA4 revealed the presence of motifs typical of cysteine proteases. BLASTx searches displayed a high degree of identity to dsRNA4 from other members of the *Chrysoviridae* family (the highest identity was to DsCV1 putative protease with 66.11 % identity). The ovarian tumour (OTU) conserved domain of cysteine protease cd22754 (E-value 6.11e-05) was found in dsRNA 4 spanning from 2505 to 2639 bp. The OUT domain is a member of the superfamily cl45892 and has also been detected in other chrysoviruses (Shahi et al., 2021; Zhai et al., 2018).

The dsRNA screening showed that one of the fungal isolates from Slovenia (labelled PIŠ 3.16) could also be infected with a chrysovirus, which was confirmed by HTS and designated as Dothistroma septosporum chrysovirus 3 (DsCV3). The genome of the DsCV3 has a four dsRNA segment organisation, presented in Fig. 1B. Length of the DsCV3 dsRNA1 is 3648 bp (GC content 45.35 %), and it has a single long ORF that codes for 1095 aa long protein (126.36 kDa). CDD search discovered the same conserved domain pfam021123 (RdRp_4; E-value 2.56e-66) from 1264 to 2625 bp in DsCV3 dsRNA1. dsRNA2 is 3453 bp long (GC content 48.03 %) and has two ORFs, which potentially encode 141 (P3S) and 852 aa (P3) proteins, with a molecular mass of 15.80 kDa and 95.83 kDa, respectively. Sequence analysis of DsCV3 dsRNAs 3 showed 3072 bp (GC content 47.86 %). DsCV3 dsRNA3 contains a single large ORF encoding 938 aa-protein with a calculated molecular mass of 104.48 kDa. The smallest segment of DsCV3, the dsRNA4, is 2793 bp long. It has a single ORF, which codes for 846 aa protein (93.58 kDa). No conserved domains were detected in DsCV3 dsRNA4. The BLASTx search with DSCV3 genome segments sequences as a query detected counterpart proteins encoded by other chrysoviruses. The first hit was proteins of DsCV1, with an identity of 96.26, 93.19, 95.95 and 97.75 %, respectively, for each dsRNA. It has been observed that the 5′ end untranslated regions (UTRs) of dsRNAs 1–4 of both studied chrysoviruses possess a highly conserved region of approximately 45 nucleotides (nt), analogous to the "box 1″ found in most chrysoviruses, as well as a second region containing numerous CAA repeats located downstream from "box 1″, similar to the enhancer elements found in the 5′-UTRs of tobamoviruses (Gallie and Walbot, 1992; Kotta-Loizou et al., 2020), as can be seen in Supplementary Figure S1. In RdRps encoded by dsRNA1 of both viruses, eight conserved motifs typically present in RdRps of eukaryotic dsRNA viruses (Bruenn, 1993) have been detected (Supplementary Figure S2).

The ML phylogenetic analyses of RdRp aa sequences of here described dsRNA viruses and related viruses (Fig. 2) have placed DsCV2 and DsCV3 within the genus *Alphachrysovirus* with the closest relationship with the DsCV1 (Shah et al., 2023), the first reported virus infecting *D. septosporum*. DsCV1–3 nested in a very well-supported cluster closely related to viruses with non-specified hosts, Grapevine associated chrysovirus 1 (Rwahnih et al., 2011) and Erysiphe necator associated chrysovirus 3 (Rodriguez-Romero et al., unpublished), but also interestingly, with viruses infecting entomopathogenic fungi Isaria javanica chrysovirus 1 (Herrero, 2017) and Beauveria bassiana chrysovirus 1 (Gilbert et al., 2019).

Taking all these results together, the PASC values (Supplementary Tables S6-S12) and the species demarcation criteria given by ICTV in the genus *Alphachrysovirus* (nucleotide and deduced amino acid sequence data, $\leq$ 70 % and $\leq$ 53 % aa sequence identity in the RdRp and CP, respectively), it can be proposed that DsCV1, 2 and 3 might be considered as variants of the newly proposed species by Shah et al. (2023). Although DsCV2 can be considered distinct almost as another species, DsCV3 is highly similar to the DsCV1.

The Slovenian *D. septosporum* isolate PIŠ 3.16, together with two Italian isolates, are the hosts to another putative dsRNA virus. Analysis of assembled contigs via BLASTx revealed that two of them are affiliated with the dsRNA1 and dsRNA2 genome segments of known members of the genus *Gammapartitivirus* in the family *Partitiviridae*. The genome of the putative novel partitivirus, herein designated as Dothistroma septosporum partitivirus 1 (DsPV1), is composed of two linear double-stranded RNA segments of 1807 and 1572 bp, respectively (Fig. 1C). Analysis of the two genome segments revealed that the larger segment (dsRNA1) encodes a putative RdRp of 539 aa (predicted molecular weight of 62.66 kDa). In comparison, the smaller segment encodes a putative CP of 434 amino acids (predicted molecular weight of 46.46 kDa). The GC contents of the RdRp and CP encoding genome segments were found to be 49.03 % and 51.59 %, respectively. According to NCBI BLASTx searches, DsPV1 shares 76.95 % RdRp aa identity with Penicillium stoloniferum virus S (PsVS) (Kim et al., 2003), while the

Table 1
Identification of putative viruses found in *Dothistroma* spp. isolates based on BLASTX search and their genome organization.

Acronym	Genomic segment/ORF (function)	Length[1] (nt)	GenBank[2]	Putative family (genus)[3]	BLASTx first hit[4]	Reference (GenBank accession)	E value	QC (%)[5]	I(%)[6]	Average read length	Reads	Depth of coverage
DsCV2	dsRNA1 (RdRp)	3417	OR827032	*Chrysoviridae* (*Alphachrysovirus*)	Dothistroma septosporum chrysovirus 1 (RdRp)	Shah et al., 2023 (CAI9240336)	0.0	95	72.26	152	35,802	1593
	dsRNA2 (P3)	3314	OR827033		Dothistroma septosporum chrysovirus 1 (hypothetical protein)	Shah et al., 2023 (CAI9240338)	0.0	74	48.47	152	43,731	2006
	dsRNA3 (CP)	3180	OR827034		Dothistroma septosporum chrysovirus 1 (capsid protein)	Shah et al., 2023 (CAI9240339)	0.0	91	53.62	152	66,519	3180
	dsRNA4 (Protease)	2866	OR827035		Dothistroma septosporum chrysovirus 1 (putative protease)	Shah et al., 2023 (CAI9240340)	0.0	88	66.11	152	89,007	4721
DsCV3	dsRNA1 (RdRp)	3648	OR827036	*Chrysoviridae* (*Alphachrysovirus*)	Dothistroma septosporum chrysovirus 1 (RdRp)	Shah et al., 2023 (CAI9240336)	0.0	90	96.26	150	37,176	1529
	dsRNA2 (P3)	3453	OR827037		Dothistroma septosporum chrysovirus 1 (hypothetical protein)	Shah et al., 2023 (CAI9240338)	0.0	74	93.19	150	31,968	1389
	dsRNA3 (CP)	3072	OR827038		Dothistroma septosporum chrysovirus 1 (capsid protein)	Shah et al., 2023 (CAI9240339)	0.0	91	95.95	150	46,810	2286
	dsRNA4 (Protease)	2793	OR827039		Dothistroma septosporum chrysovirus 1 (putative protease)	Shah et al., 2023 (CAI9240340)	0.0	90	97.75	150	77,460	4160
DsPV1	dsRNA1 (RdRp)	1807	OR827040	*Partitiviridae* (*Gammapartitivirus*)	Penicillium stoloniferum virus S (RdRp)	Kim et al., 2003 (YP_052856)	0.0	89	76.95	150	857,219	71,158
	dsRNA2 (CP)	1572	OR827041		Penicillium digitatum partitivirus 1	Gilbert et al., 2019 (AZT88595)	3e-143	82	56.35	150	665,747	61,265
DsGFV1 (9588 nt)	ORF1 (REP)	5682	OR827029	*Gammaflexiviridae*	Pistacia-associated flexivirus 1 (replicase)	Park et al., 2020 (YP_010799909)	0.0	99	51.70	152	227,829	3612
	ORF2 (MP)	2439			Pistacia-associated flexivirus 1 (movement protein)	Park et al., 2020 (YP_010799910)	0.0	84	62.15			
	ORF3 (HP)	984			Pistacia-associated flexivirus 1 (hypothetical protein)	Park et al., 2020 (YP_010799911)	6e-127	96	60.44			
DpNV1	RdRp	3268	OR827027	*Narnaviridae*	Neofusicoccum parvum narnavirus 1 (RdRp)	Cao et al., unpublished (WAK75250)	0.0	93	50.73	152	444,215	20,661
DsNV1	RdRp	3382	OR827028	*Narnaviridae*	Erysiphe necator associated narnavirus 22 (RdRp)	Rodriguez-Romero et al. unpublished (QJT93754)	0.0	94	47.48	150	3129	139
DsMV1 (3619 nt)	RNA1 (RdRp)	6289	OR827030	*Mymonaviridae* (*Penicillimonavirus*)	Cercospora beticola negative-stranded virus 3 (RdRp)	Li et al., 2021 (UVB78667)	0.0	93	70.85	152	146,563	3542
	RNA2 (ORF1)	741	OR827031		Plasmopara viticola lesion associated mononegaambi virus 6 (hypothetical protein)	Forgia et al., unpublished (WKE35276)	1e-39	72	42.62	152	128,546	5399
	RNA2 (ORF2)	1182			Plasmopara viticola lesion associated mononegaambi virus 5 (hypothetical protein)	Forgia et al., unpublished (WKE35273)	0.0	98	74.81			
	RNA2 (ORF3)	603			Plasmopara viticola lesion associated mononegaambi virus 6 (hypothetical protein)	Forgia et al., unpublished (WKE35278)	1e-70	92	57.84			
	RNA2 (ORF4)	636			Plasmopara viticola lesion associated mononegaambi virus 6 (hypothetical protein)	Forgia et al., unpublished (WKE35279)	2e-06	36	42.50			
DsBLV1	L (RdRp)	6515	OR827042	*Discoviridae*	Erysiphe necator associated negative-stranded RNA virus 4 (RdRp)	Rodriguez-Romero et al., unpublished (QJW70357)	0.0	97	85.96	152	226,116	5322
	M (NS)	1305	OR827043		Cercospora beticola negative-stranded virus 5 (NS)	Li et al., 2021 (UVB78672)	7e-41	34	48.08	152	61,455	7158
	S (NC)	1201	OR827044		Penicillium discovirus (nucleocapsid)	Rrishnamurthy et al., unpublished (YP_010840287)	1e-82	64	53.28	152	167,474	21,196

(*continued on next page*)

Table 1 (*continued*)

Acronym	Genomic segment/ORF (function)	Length[1] (nt)	GenBank[2]	Putative family (genus)[3]	BLASTx first hit[4]	Reference (GenBank accession)	E value	QC (%)[5]	I(%)[6]	Average read length	Reads	Depth of coverage
DsBLV2	L (RdRp)	6619	OR827045	*Discoviridae*	Plasmopara viticola lesion associated mycobunyavirales-like virus 5 (RdRp)	Chiapello et al., 2020 (QGY72642)	0.0	81	61.32	152	90,888	2087
	M (NS)	1279	OR827046		Rice dwarf-associated bunya-like virus (nonstructural protein)	Wang et al., 2022 (UTJ93942)	5e-26	52	33.48	152	130,733	15,088
	S (NC)	1227	OR827047		Penicillium discovirus (nucleocapsid)	Rrishnamurthy et al., unpublished (YP_010840287)	1e-63	52	48.60	152	39,965	4951
DsBLV3	L (RdRp)	6465	OR827048	*Discoviridae*	Erysiphe necator associated negative-stranded RNA virus 4 (RdRp)	Rodriguez-Romero et al., unpublished (QJW70357)	0.0	97	86.06	152	11,274	265
	M (NS)	1199	OR827049		Cercospora beticola negative-stranded virus 5 (NS)	Li et al., 2021 (UVB78672)	1e-41	36	48.00	152	30,479	3864
	S (NC)	1117	OR827050		Penicillium discovirus (nucleocapsid)	Rrishnamurthy et al., unpublished (YP_010840287)	5e-83	69	53.67	152	6368	842
DsBLV4	L (RdRp)	6469	OR827051	*Discoviridae*	Erysiphe necator associated negative-stranded RNA virus 4 (RdRp)	Rodriguez-Romero et al., unpublished (QJW70357)	0.0	97	86.15	150	82,871	1922
	M (NS)	1275	OR827052		Cercospora beticola negative-stranded virus 5 (NS)	Li et al., 2021 (UVB78672)	4e-41	35	47.37	150	145,610	17,131
	S (NC)	1189	OR827053		Penicillium discovirus (nucleocapsid)	Rrishnamurthy et al., unpublished (YP_010840287)	5e-82	65	52.90	150	68,391	8628
DsBLV5	L (RdRp)	6551	OR827054	*Discoviridae*	Cercospora beticola negative-stranded virus 2 (RdRp)	Li et al., 2021 (UVB78666)	0.0	97	73.53	150	325,371	7450
	M (NS)	1758	OR827055		Cercospora beticola negative-stranded virus 4–3 (NS)	Li et al., 2021 (UVB78671)	0.0	87	63.69	150	20,716	1768
	S (NC)	1124	OR827056		Cercospora beticola negative-stranded virus 4–2 (NC)	Li et al., 2021 (UVB78669)	1e-155	77	75.17	150	1116,540	149,004
DsBLV6	L (RdRp)	6552	OR827057	*Discoviridae*	Plasmopara viticola lesion associated mycobunyavirales-like virus 5 (RdRp)	Chiapello et al., 2020 (QGY72642)	0.0	82	61.04	150	104,016	2381
	M (NS)	1254	OR827058		Rice dwarf-associated bunya-like virus (nonstructural protein)	Wang et al., 2022 (UTJ93942)	5e-27	53	34.22	150	94,496	11,303
	S (NC)	1200	OR827059		Penicillium discovirus (nucleocapsid)	Rodriguez-Romero et al., unpublished (QJW70357)	2e-64	53	48.60	150	26,699	3337

[1] Virus sequence length obtained by SPAdes assembly.
[2] GenBank accession number of each virus.
[3] Placment of the viruses according to their genome organisation and phylogenetic analysis.
[4] The most similar virus based on BLASTX search against the NCBL protein sequence database (date of the last search November 2023).
[5] Query cover.
[6] Identity.

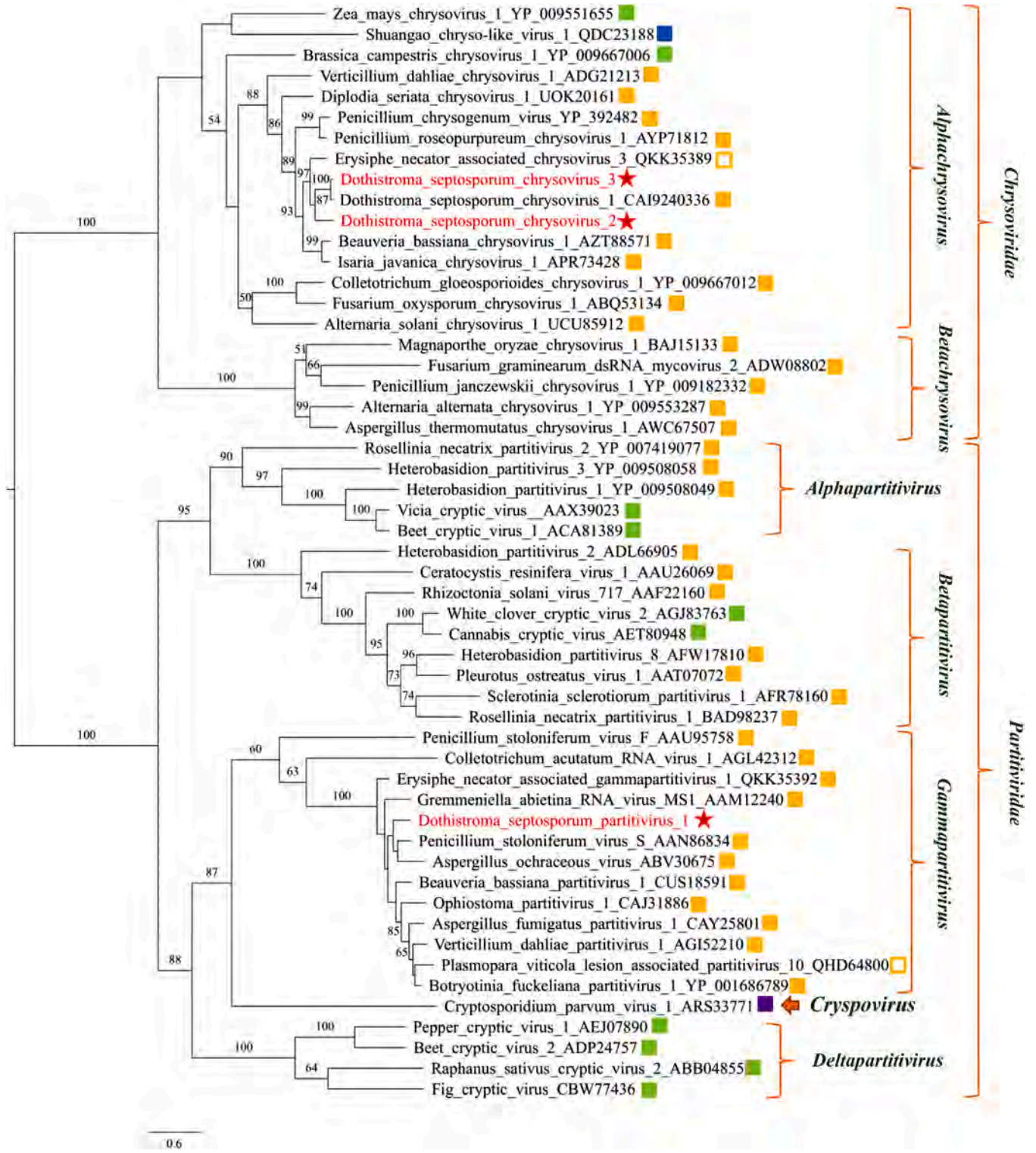

Fig. 2. The ML (RAxML) phylogenetic analysis based on the predicted RdRp of dsRNA viruses from the present study (indicated in red and by a red asterisk) and selected members of related taxa with GenBank accession numbers. Nodes were labelled with bootstrap support values of ≥50 %. Branch lengths were scaled to the expected underlying number of amino acid substitutions per site, and the tree was rooted at the midpoint. The family and genera classification was shown behind braces, and colourful squares represented the virus-host kingdom or phylum: Fungi, Planta, Arthropoda and Apicomplexa. Open shapes point out non-specified hosts.

predicted CP of DsPV1 is most similar (identity 56.35 %) to that of Penicillium digitatum partitivirus 1 (PdPV1) (Gilbert et al., 2019). Conserved domain RdRp_1 (pfam00680; E-value 2.55e-85) member of RT_like superfamily cl02808 was detected in dsRNA1 spanning from 187 to 1521 bp.

The phylogenetic tree generated by ML analysis (Fig. 2) indicated that the putative RdRp encoded by DsPV1 was related to those of viruses within the genus *Gammapartitivirus*, family *Partitiviridae* (Fig. 2), with

PsVS and Aspergillus ochraceus virus (AoV) (Liu et al., 2008) being most closely related. It has been established that all members of the genus *Gammapartitivirus* infect ascomycetous fungi, which are usually latent infections (Vainio et al., 2018a). Given its host, genome size, organisation and phylogenetic placement, DsPV1 is the new member of the genus. Following the established partitivirus species demarcation criteria within genus *Gammapartitivirus*, <70 % aa sequence identity in the RdRp and ≤ 80 % aa sequence identity in the CP to representatives of already recognised species, we propose that DsPV1 should be considered a new species.

3.3.2. *(-)ssRNA viruses*

A decade after the first report of the potential (-)ssRNA viruses found in a fungus (Kondo et al., 2013), an immense diversity of (-)ssRNA mycoviruses has been reported (Chiapello et al., 2020; Forgia et al., 2022; Li et al., 2021; Lin et al., 2019; Liu et al., 2014; Nerva et al., 2019a, 2019b; Shamsi et al., 2022). The order *Bunyavirales* is one of the most extensive groups of segmented (-)ssRNA viruses, with 14 families recognised by the ICTV in addition to numerous unclassified bunyaviruses. Bunyaviruses are enveloped viruses, typically possessing three genome segments: the small (S), the medium (M) and the large (L) segment. The S RNA encodes the nucleocapsid protein, while the M and L segments encode the glycoproteins and the RdRp, respectively. The RdRp, in conjunction with the nucleoproteins (NPs), assembles a ribonucleoprotein (RNP) on each genomic segment. RNP complex is essential for replication and gene transcriptions (Boshra, 2022; Ferron et al., 2017; Leventhal et al., 2021; Wichgers Schreur et al., 2018). From our data, we dug out 18 contigs resembling bunyavirus genome segments, 9 of each in both RNA pools. Six were identified as L genome segments of bunyaviruses coding for RdRp, while the rest code for the proteins typical of M and S segments. Analysis of the sequence revealed that all six bunyavirus-like L genome segment sequences contained conserved regions belonging to pfam04196 Bunyavirus RdRp, the sole member of the superfamily cl20265. Specifically, DsBLV1 had a conserved region spanning from nt 1849 to 3849 (E-value 3.61e-18); DsBLV2 from nt 2175 to 3776 (E-value 5.83e-15); DsBLV3 from nt 1826 to 3826 (E-value: 7.26e-16); DsBLV4 from 1819 to 3819 nt (E-value: 1.29e-15); DsBLV5 1765–3771 nt (E-value: 5.97e-18); and DsBLV6 from nt 2133–3734 (E-value: 9.60e-17). No conserved regions were found in sequences M and S genome segments of putative new bunya-like viruses. Based on the results of the RT-PCR screening and PASC analyses (Supplementary Table S13-S18), we associated the M and S segments with their respective L segments. DsBLV1–4 was simple enough since they, based on RT-PCR results, infect only one fungal isolate (Supplementary Table S1). Finally, we linked the unassigned genome segments to each other by comparing the similarity identity of their sequences with sequences of already organised genomes. Genome organisations of DsBLV1–6 are illustrated in Fig. 3. An ML phylogenetic analysis based on multiple alignments of the RdRp amino acid sequences of six bunya-like viruses from the present study and other viruses from the *Bunyavirales* and *Mononegavirales* (as an outgroup) was conducted (Fig. 4). The phylogenetic analysis revealed that DsBLV1–6 clustered with members of *Discoviridae*, a newly established family within the *Bunyavirales*. DsBLV1, DsBLV3 and DsBLV4 formed a very well-supported cluster together with Erysiphe necator associated negative-stranded RNA virus 4 (unpublished). DsBLV2 and DsBLV6 formed a joint group closely related to the Plasmopara viticola lesion associated mycobunyavirales-like virus 5 (Chiapello et al., 2020). While DsBLV5

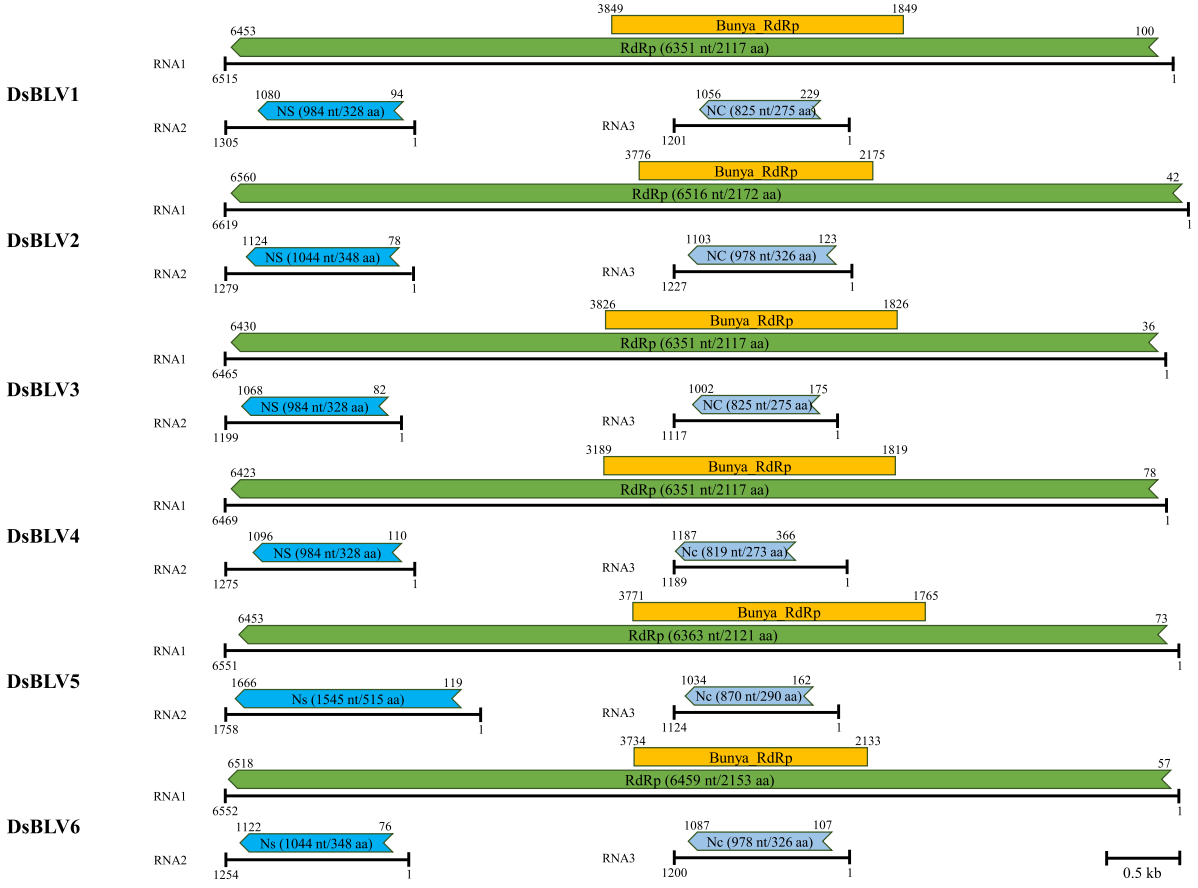

Fig. 3. Genome organization of Dothistroma bunya-like viruses 1 to 6 (DsBLV1–6). Open reading frames are represented with arrows (RdRp=RNA dependent RNA polymerase; NS= non-structural protein; NC=Nucleocapsid; nt=nucleotides; aa=amino acids). Conserved domains of Bunyavirus RdRp, found in L genome segments of DsB-LV1–6, are characterized in yellow boxes.

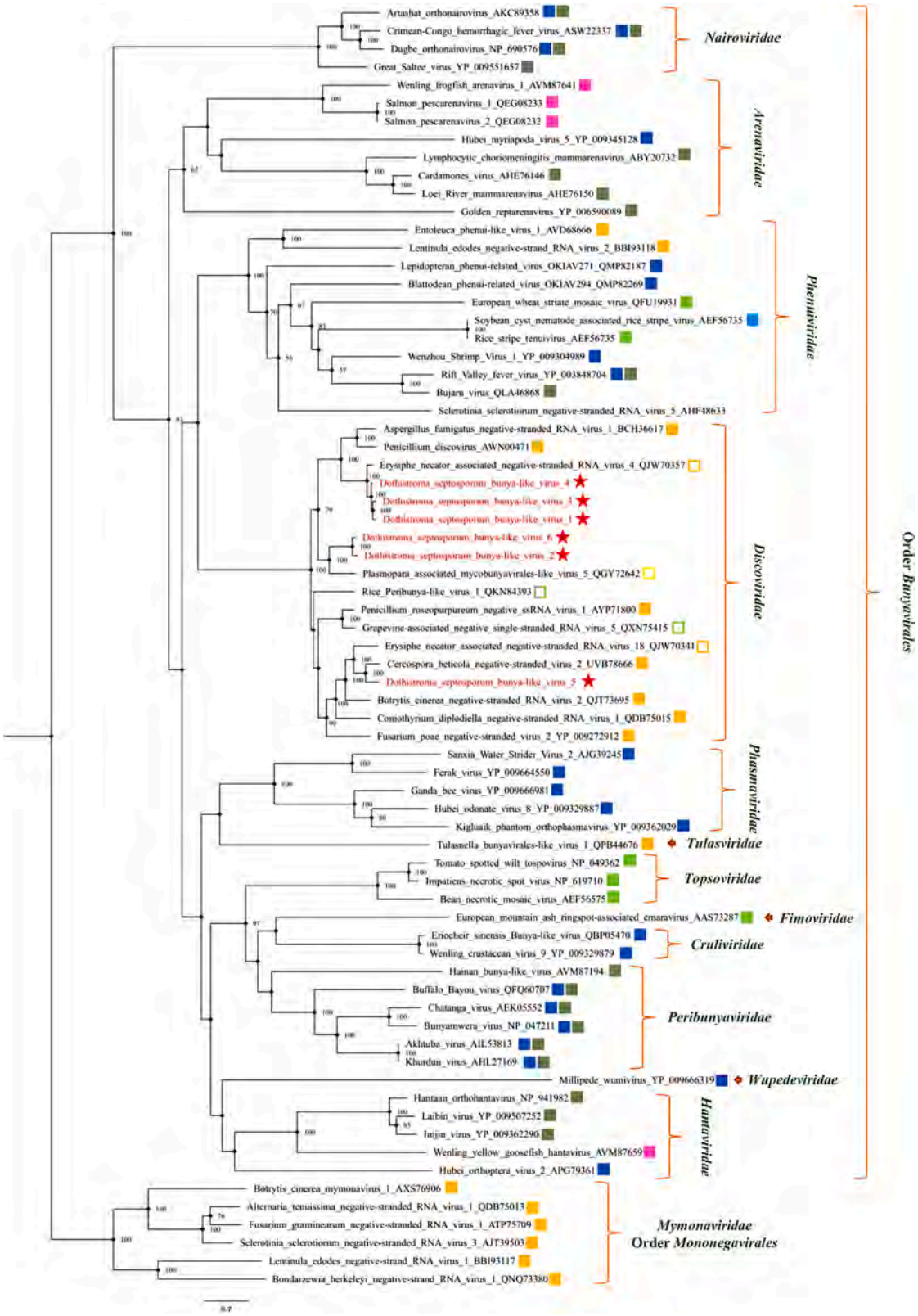

Fig. 4. Phylogenetic placement of bunyaviruses described in the current study (indicated in red and by ★). The tree focuses on the order *Bunyavirales,* with viruses of the family *Mymnoviridae* used as an outgroup. Only bootstrap values above 50 % are indicated. Scale bar = 0.7 expected changes per site per branch. Kingdom or phylum of the viral host are represented by colourful squares: Mammalia, Chordata, Arthropoda, Fungi, Planta, Nematoda, and open shapes indicate a non-specified host.

appears more distantly related to the former ones, nesting on a separate branch in the family *Discoviridae*, with Cercospora beticola negative-stranded virus 2 (Li et al., 2021) as the most closely related virus.

The order *Mononegavirales* consists of 11 viral families with non-segmented, linear, single-stranded negative-sense RNA genomes (Afonso et al., 2016), or that was believed until recently. The family *Mymonaviridae* is the only one recognised to host mycoviruses. Some family members have been indicated to induce hypovirulence in the fungal host (Jiāng et al., 2019). Sequence analysis of the 6257 nt long contig (GC content 44.97 %) revealed a single large antisense ORF coding a 1956 aa protein (221.30 kDa). A consecutive BLASTx search of the protein revealed its relation with RdRps of *Mononegavirales* members, with the first two results being Cercospora beticola negative-stranded virus 3 (Li et al., 2021) and Plasmopara viticola lesion-associated mononegaambi virus 5 (Chiapello et al., 2020). Hence, we characterised this new putative virus as Dothistroma septosporum mononegaambivirus 1 (DsMNAV1). Two conserved regions were detected in the putative RdRp aa sequence. A larger one spanning from 765 to 3260 nt belongs to pfam00946 (E-value: 7.52e-94), the sole member of superfamily cl15638, characteristic of Mononegavirales RdRp. The second conserved domain is the Mononegavirales mRNA-capping region V (pfam14318; E-value: 3.84e-11), spanning from 3297 to 3896 nt. It has been discovered that the V domain is indispensable for forming an mRNA cap. Phylogenetic analysis of the RdRp protein sequence shows that DsMNAV1 is closely related to the *Penicillimonavirus* genus (Fig. 5C). Surprisingly, a more recent examination of the HTS data exposed another contig analogous to those of the mymonaviruses. The sequence analysis of the said contig showed that it is 3691 nucleotides in length, and it hosts four ORFs that mainly coded for proteins of unknown function, except for the one that coded for the putative NC, located in the second to last position of the antisense strand. The BLASTp search results of the putative proteins matched them with the group of NS proteins coded by the second RNA segment of recently described bipartite members of the *Mymonaviridae* family (Pagnoni et al., 2023). Following PCR amplification with a primer pair spanning the junction of DsMNAV1 RNA segments, no amplification product consistent with a monopartite genome organisation was obtained, thereby confirming the potential for an unusual bipartite genome organisation of DsMNAV1 as shown in Fig. 5A. Additionally, in the second RNA segment conserved noncoding sequences were identified to be located downstream of each ORF (Fig. 5B). It is a common occurrence to observe gene-junction sequences in the viral genome, which is a characteristic feature of mononegaviruses (Liu et al., 2014). To further strengthen the hypothesis that DsMNAV1 may be a bisegmented virus, we observed significant conservation in the UTRs of the two RNA segments, particularly at the 3′ end, as illustrated in Fig. 5D.

3.3.3. (+)ssRNA viruses

As stated by the ICTV, the order of (+)ssRNA viruses *Tymovirales* encompasses five families (*Alpha-, Beta-, Delta- and Gammaflexiviridae* and *Tymoviridae*), which primarily infect plant hosts; however, a few members of the *Tymovirales* have been noted to have either fungal or insect hosts. The majority of mycoviruses from the order *Tymovirales* have been classified into the *Gammaflexiviridae* family, with Botrytis virus F (BVF) being first described (Howitt et al., 2001). BVF is a monopartite positive-sense single-stranded RNA virus with a genome length of ca. 6.8 kb. It has two ORFs encoding a replication-associated protein (REP) and CP. The RdRp domain is expressed through a read-through translation strategy exclusive to the *Tymovirales* order (Howitt et al., 2001; Svanella-Dumas et al., 2018). The largest *de novo* assembled contig from our raw RNA-seq data was 9588 nt long. Sequence analyses predicted three positive-sense ORFs coding for proteins P1 (1894 aa; 208.86 kDa), P2 (813 aa; 88.54 kDa) and P3 (328 aa; 36.35 kDa), respectively (Fig. 6A.). BLASTp search related these putative proteins with proteins characteristically encoded by viruses from the *Gammaflexiviridae*. The P1 protein has a signature of REP, P2 resembles movement protein (MP), and P3 is a hypothetical protein (HP) of unknown function. In cases of all three proteins, the best result in the BLASTx search was proteins coded by Pistacia-associated flexivirus 1 (PAFV1) (Park et al., 2020). Thus, we designated this new putative virus as Dothistroma septosporum gammaflexivirus 1 (DsGFV1). In the ORF1 sequence, three conserved domains were detected: viral methyltransferase (pfam01660; E-value: 1.64e-33), viral RNA helicase (pfam01443, superfamily cl26263; E-value:9.39e-22) and conserved catalytic core domain of RdRp from the (+)ssRNA viruses and closely related viruses (cd23249 member of superfamily cl40470; E-value: 1.31e-152). The sequence of the second ORF has conserved domain smart00487 (E-value: 1.34e-07), a member of the DEAD-box helicase superfamily (cl28899), a diverse family of proteins involved in ATP-dependent RNA or DNA unwinding. The ML phylogenetic analysis of the predicted REP of DsGFV1 and those of other members of the order *Tymovirales* positioned DsGFV1 into a clade together with other members of the *Gammaflexiviridae* (Fig. 6B). Not surprisingly, it forms a subclade with PAFV1, but also with other gammaflexiviruses with similar genomic organisation, as Entoleuca gammaflexivirus 1 (Velasco et al., 2019) and Leucocoprinus gammaflexivirus C (Jo and Cho, unpublished).

The family *Narnaviridae* was recently reclassified into two distinct families, with the mitoviruses being split off into a new family, *Mitoviridae*, as ratified by the ICTV Executive Committee in 2019. Presently, there are only two classified species within the family *Narnaviridae*. However, numerous narnaviruses have been recently reported in fungi and oomycetes (Li et al., 2021; Osaki et al., 2016; Raco et al., 2022). Additionally, several novel groups of narna-like viruses with unique genome organisations have been recently uncovered (Chiapello et al., 2020; Chiba et al., 2021; Dinan et al., 2020; Jia et al., 2021; Ruiz-Padilla et al., 2021; Sutela et al., 2020).

In this study, two contigs (3268 and 3382 nt long), one of each in both RNA pools, contained a single complete ORF encoding putative proteins of 1021 and 1071 aa, respectively, as it can be seen in Fig. 7A. A BLASTx search of the deduced proteins revealed their similarity to the RdRps coded by the representative members of the *Narnaviridae* family. The contig from the first RNA library shared the highest sequence similarity with Neofusicoccum parvum narnavirus 1 (NpNV1) (Nerva et al., 2019b), while the one from the second RNA library was closest to Erysiphe necator-associated narnavirus 22 (EnANV22) (Rodriguez-Romero et al., unpublished). Interestingly, RT-PCR screening revealed that the narna-like from the RNA pool 1 infects the only isolate of *D. pini* used in this study. Hence, we characterised this new putative virus as Dothistroma pini nanrnavirus 1 (DpNV1). Supposedly, this is the first virus reported to infect *D. pini*. The contig assembled from the second RNA pool was found to infect one of the Irish isolates of *D. septosporum*. Thus, it was named Dothistroma septosporum narnavirus 1 (DsNV1). CDD search discovered conserved catalytic core domain of RdRp from the positive-sense single-stranded RNA viruses (superfamily cl40470 member cd23183; E-value: 1.09e-07) in ORF of the DsNV1 but not in DpNV1. Nevertheless, when the cores RdRp region of both viruses were aligned with other narnaviruses (Supplementary Figure. S6), the seven RdRp motifs were observed. To clarify the relationship between the new two putative narnaviruses and the other members of the *Narnaviridae*, an ML phylogenetic tree (Fig. 7B) was generated based on multiple alignments of full-length RdRp aa sequences. The ML tree shows that DpNV1 and DsNV1 cluster with narnaviruses. DsNV1 is phylogenetically close to EnANV22 and Monilinia narnavirus H (Jo and Cho, unpublished). On the other hand, DpNV1 clustered in a seemingly distant group of the prior, closely related to NpNV1, Plasmopara viticola lesion-associated narnavirus 14 (Chiapello et al., 2020) and Erysiphe necator associated narnavirus 48 (Rodriguez-Romero et al., unpublished).

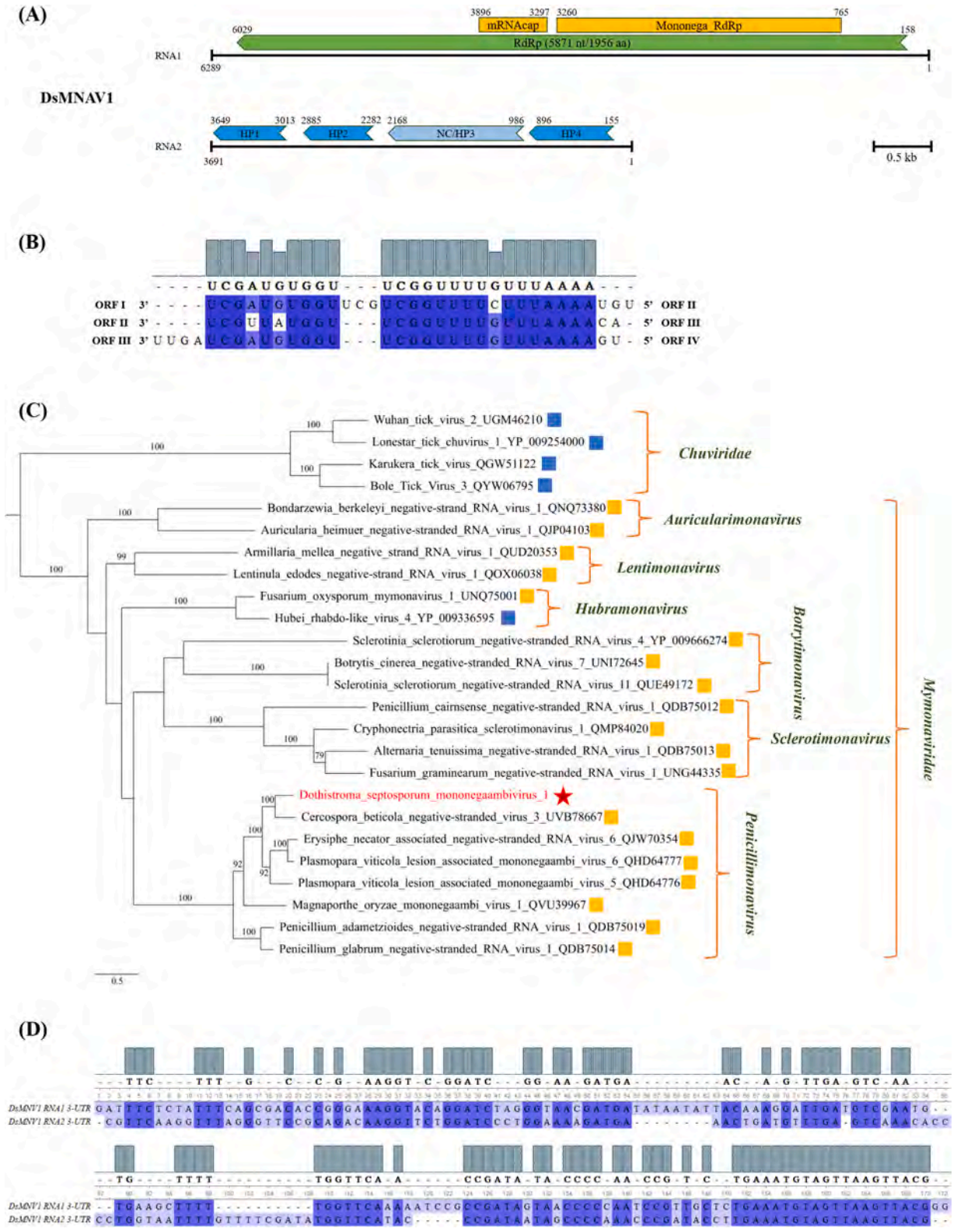

Fig. 5. (A) Genome organisation of the Dothistroma septosporum mononegaambivirus 1 (DsMV1) with important nucleotides and amino acids. ORFs are presented as an arrow and conserved regions by yellow boxes. (B) Alignment of the putative gene-junction sequences between ORFs in a 3′→5′ orientation of DsMNAV1. The level of consensus is represented in blue (the darker the colour, the higher the consensus) and by bars above the alignment. (C) Maximum likelihood tree (RAxML) portraying the phylogenetic relationship of the predicted RdRp of DsMNAV1 with other complete RdRp belonging to related viruses from the family *Mymonaviridae*. Branch lengths present the calculated evolutionary distance and are scaled to the expected underlying number of amino acid substitutions per site. Nodes are marked with bootstrap percentages ≥50 %. Genera classification and the GeneBank accession codes are next to the virus names. ★ indicates DsMV1. Biological classification of the hosts: Fungi, Arthropoda. (D) MUSCLE alignment of 3-UTRs of RNA1 and RNA2 segments of DsMNAV1. The level of conservation is presented as bars above the alignment.

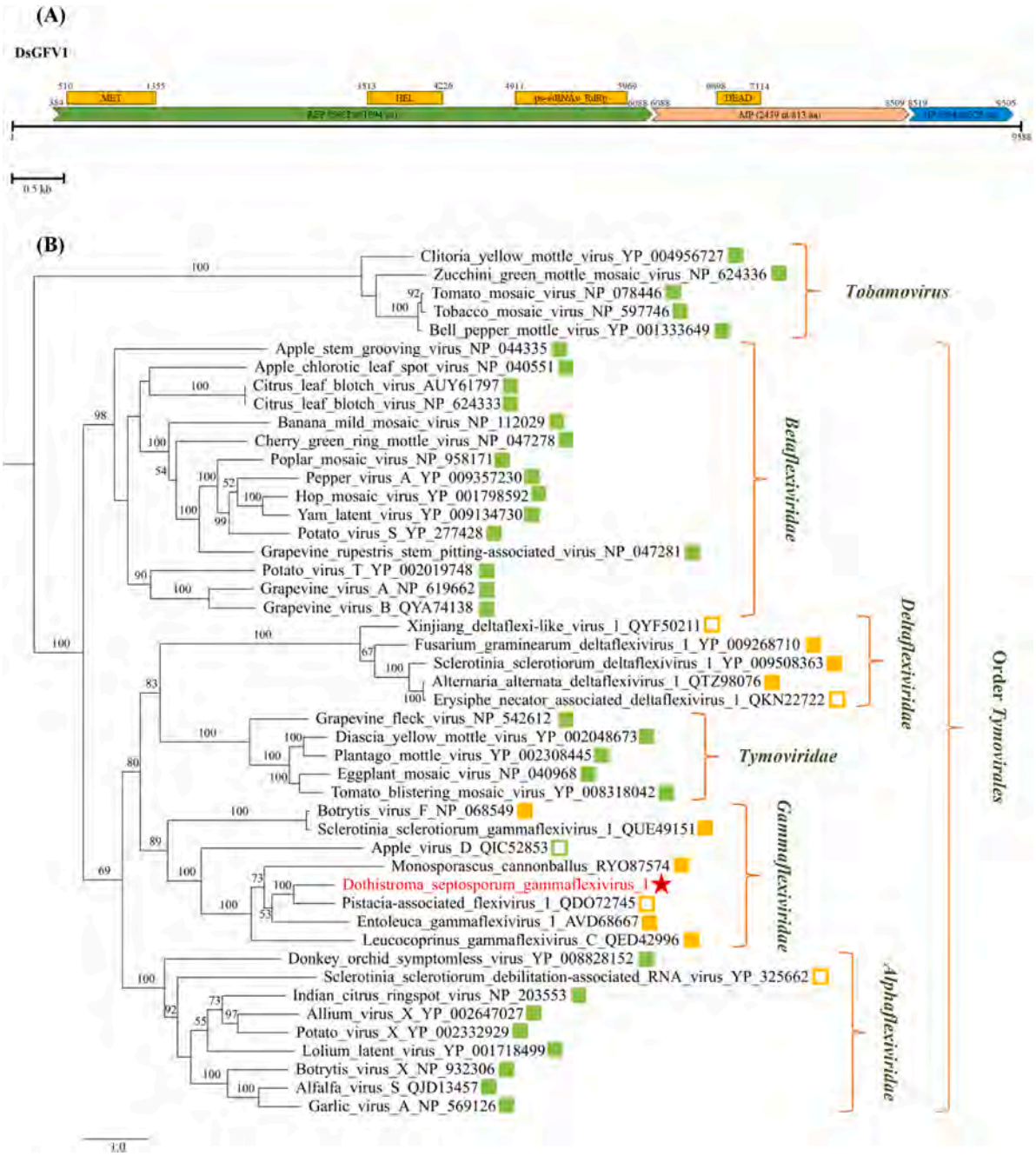

Fig. 6. (A) Graphic representation of Dothistroma septosporum gammaflexivirus 1 (DsGFV1). Arrows indicate open reading frames (ORFs), and yellow rectangular boxes are for conserved domains (MET=viral methyltransferase; HEL=viral RNA helicase; ps-ss RdRp=conserved catalytic core domain of RNA-dependent RNA polymerase from the positive-sense single-stranded RNA viruses and closely related viruses; DEAD=DEAD-like helicase). (REP=replication-associated protein; MP=moving protein; HP=hypothetical protein; nt=nucleotides; aa=amino acids). (B) The maximum likelihood phylogenetic tree based on REP sequences of DsGFV1 (in red and tagged with ★) with other classified members of the order *Tymovirales*. Viruses from the genus *Tobamovirus* were used as an outgroup. Nodes are labelled with bootstrap support values ≥50 % only. Branch lengths are scaled to the expected underlying number of amino acid substitutions per site. Scale bar=1.0 expected changes per site per branch. The tree is rooted in the midpoint. Biological classification of the hosts: Fungi, Planta, open shapes indicate an unassigned host.

3.4. Virus diversity and multiple infections in Dothistroma isolates

RT-PCR confirmed the specific fungal host isolates for each putative virus. In RNA pool 1 (do1), three isolates of *D. septosporum* and one of *D. pini* have shown the presence of mycoviruses (36 %), and in the case of the second RNA pool (do2), five *D. septosporum* isolates were infected (50 %). As mentioned, four isolates (two of *D. septosporum* in each pool) were infected with multiple, evolutionarily distinct viruses (see Supplementary Table S1). Viral co-infections are not rare in fungi (Arjona-Lopez et al., 2018; Botella and Hantula, 2018; Hantula et al., 2020; Osaki et al., 2016; Ran et al., 2016; Vainio and Sutela, 2020; Zhang et al., 2022). It appears that viral co-infections do not depend on horizontal transmission (via anastomosis) between compatible fungal hosts, and the factors on the cellular level that determine it have been discussed by Thapa and Roossinck (2019). The accumulation of viral co-infections happens due to the ageing of the strain of the fungal host (Vainio et al., 2015c). If we consider its Eurasian origin (Mullett et al., 2021) that could be the case with *D. septosporum*. We could propose that the isolates showing multiple viral infections have been present in the localities where they have been collected long enough to hoard multiple

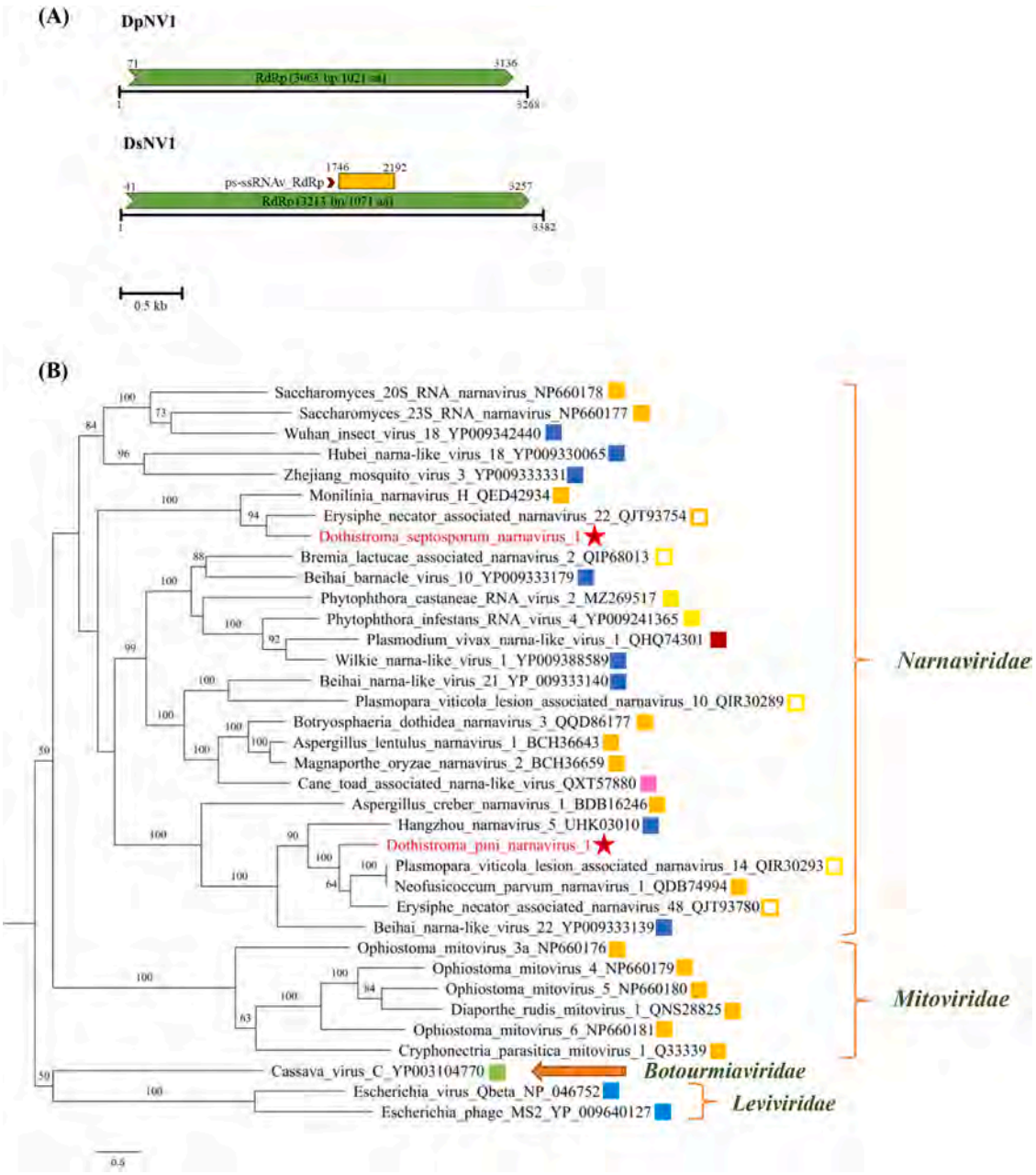

Fig. 7. (A) Genome organisation of two narnaviruses from this study, Dothistroma pini narnavirus 1 (DpNV1) and Dothistroma septosporum narnavirus 1 (DsNV1). (B) ML phylogenetic tree based on the amino acid sequences of putative RdRp of two narnaviruses found in this study (indicated by ★), and other members of the *Narnaviridae* and the viruses from families *Mitoviridae, Botourmiaviridae* and *Leviviridae* available in GenBank. Nodes are labelled with bootstrap support values ≥50 %. Branch lengths are scaled to the expected underlying number of amino acid substitutions per site. The use of colourful squares depicts a representation of the Kingdom or Phylum of the Viral Host: Fungi, Oomycota, Apicomplexa, Chordata, Planta, Bacteria and open shapes indicate a non-specified host. The scale bar at the lower left corresponds to a genetic distance of 0.5.

co-infections. Vainio et al. (2015c) further suggested that co-infections by viral species that are distantly related are more enduring than those between strains of the same species and that mutual exclusion could be a factor in determining the composition of viral communities. The results of the presented study indicate that this assertion may be accurate for *D. septosporum*.

In terms of occurrence, some viruses are more prevalent than others, with DsPV1 being the most common. This gammapartitivirus appears in three *D. septosporum* isolates from two localities in Italy and Slovenia. This suggests that this virus evolved towards an optimal virus-host interaction that enabled it to replicate and move more efficiently through its host populations, as has been pointed out in other mycovirus population studies (Botella et al., 2022, 2015a; Schoebel et al., 2017; Voth et al., 2006). The efficiency of mycovirus transmission can be influenced by various factors, such as the specific interaction between the mycovirus and the host fungus, the presence of other environmental factors that affect spore dispersal, and the availability of a susceptible host (Ning et al., 2022; Vainio et al., 2013). Notably, DsCV1 and DsCV3 are very closely related, although they were found in more geographically distant hosts. Therefore, it is possible to hypothesise that the British and Slovenian populations of *D. septosporum* are more closely related than the Czech population. However, an extensive collection of fungal isolates from diverse localities should be screened to confirm this hypothesis.

3.5. DsBLV1 transmission experiment

The vertical transmission of the three genomic segments of DsBLV1 was confirmed for all three segments (RdRp, NC and NS). The transmission rate of DsBLV1 was 100 % for the L, M and S genomic segments for all 96 monosporic isolates studied (Supplementary Table S21). The alignment of 30 randomly chosen amplicons of partially amplified RdRp, NC, NS showed 100 % overall pairwise nt identity (data not shown). These results confirm that (i) this bunyavirus is readily vertically transmitted through *D. septosporum* conidia and (ii) the three RNA genomic segments are very conserved and likely necessary for DsBLV1 transmission and replication. If the presence of DsBLV1 is related to a lower or higher sporulation of *D. septosporum*, it should be further investigated. The efficiency of mycovirus transmission through asexual spores (conidia) has been commonly pointed out as very efficient. While asexual spores and sexual spores both play a role in mycovirus dissemination, their relative efficiency as transport means can depend on several factors (Hough et al., 2023). Asexual spores are generally more likely to encounter potential hosts due to their greater abundance and the wider range of dispersal mechanisms. However, sexual spores, while less numerous, may have advantages in terms of longer dispersal distances and the protection provided by specialised structures, allowing them to reach new habitats or hosts potentially, i.e. Hymenoscyphus fraxineus mitovirus 1 (HfMV1) is readily transmitted by ascospores, the primary spreading means of the *Hymenoscyphus fraxineus*, the causal agent of ash dieback (Čermáková et al., 2017; Schoebel et al., 2017).

4. Conclusions

Here, we presented the initial evidence of virus diversity in European populations of *D. septosporum* and that they are vertically transmitted. Additionally, we documented the first mycoviruses infecting *D. pini*. In the near future, these mycoviruses' characterisation and biological function might provide novel means as DNB biocontrol and expand our knowledge of the diversity, ecology, evolution, and taxonomy of mycoviruses in forest conifer pathogens.

CRediT authorship contribution statement

Miloš Trifković: Writing – original draft, Visualization, Validation, Resources, Methodology, Investigation, Funding acquisition, Formal analysis, Data curation, Conceptualization. **Ondřej Hejna:** Writing – review & editing, Methodology, Formal analysis, Data curation. **Anna Kuznetsova:** Methodology, Investigation, Formal analysis. **Martin Mullett:** Writing – review & editing, Resources, Methodology. **Libor Jankovský:** Supervision, Funding acquisition. **Leticia Botella:** Writing – review & editing, Resources, Methodology, Funding acquisition, Formal analysis, Conceptualization.

Declaration of competing interest

The authors declare that they have no known competing financial interests or personal relationships that could have appeared to influence the work reported in this paper.

Data availability

Data will be made available on request.

Acknowledgements

We are thankful to Dagmar Palovčíková and Milica Raco (both MENDELU, Czech Republic) for technical assistance. Eeva-Liisa Terhonen (LUKE, Finland) is thanked for reading and commenting on the manuscript.

Funding

This research was funded by Project Phytophthora Research Centre Reg. No CZ.02.1.01/ 0.0/0.0/15_003/0000453, co-financed by the Czech Ministry for Education, Youth and Sports and the European Regional Development Fund, and by Specific University Research Fund of the Faculty of Forestry and Wood Technology, Mendel University in Brno (grant No LDF_VP_2020063).

Supplementary materials

Supplementary material associated with this article can be found, in the online version, at doi:10.1016/j.virusres.2024.199476.

References

Afonso, C.L., Amarasinghe, G.K., Bányai, K., Bào, Y., Basler, C.F., Bavari, S., Bejerman, N., Blasdell, K.R., Briand, F.X., Briese, T., Bukreyev, A., Calisher, C.H., Chandran, K., Chéng, J., Clawson, A.N., Collins, P.L., Dietzgen, R.G., Dolnik, O., Domier, L.L., Dürrwald, R., Dye, J.M., Easton, A.J., Ebihara, H., Farkas, S.L., Freitas-Astúa, J., Formenty, P., Fouchier, R.A.M., Fù, Y., Ghedin, E., Goodin, M.M., Hewson, R., Horie, M., Hyndman, T.H., Jiāng, D., Kitajima, E.W., Kobinger, G.P., Kondo, H., Kurath, G., Lamb, R.A., Lenardon, S., Leroy, E.M., Li, C.X., Lin, X.D., Liú, L., Longdon, B., Marton, S., Maisner, A., Mühlberger, E., Netesov, S.V., Nowotny, N., Patterson, J.L., Payne, S.L., Paweska, J.T., Randall, R.E., Rima, B.K., Rota, P., Rubbenstroth, D., Schwemmle, M., Shi, M., Smither, S.J., Stenglein, M.D., Stone, D.M., Takada, A., Terregino, C., Tesh, R.B., Tian, J.H., Tomonaga, K., Tordo, N., Towner, J.S., Vasilakis, N., Verbeek, M., Volchkov, V.E., Wahl-Jensen, V., Walsh, J.A., Walker, P.J., Wang, D., Wang, L.F., Wetzel, T., Whitfield, A.E., Xiè, J., Yuen, K.Y., Zhang, Y.Z., Kuhn, J.H., 2016. Taxonomy of the order *Mononegavirales*: update 2016. Arch. Virol. 161, 2351–2360. https://doi.org/10.1007/s00705-016-2880-1.

Altschul, S.F., Gish, W., Miller, W., Myers, E.W., Lipman, D.J., 1990. Basic local alignment search tool. J. Mol. Biol. 215, 403–410. https://doi.org/10.1016/S0022-2836(05)80360-2.

Anagnostakis, S.L., 1982. Biological control of chestnut blight. Science (80-.). 215, 466–471. https://doi.org/10.1126/science.215.4532.466.

Arjona-Lopez, J.M., Telengech, P., Jamal, A., Hisano, S., Kondo, H., Yelin, M.D., Arjona-Girona, I., Kanematsu, S., Lopez-Herrera, C.J., Suzuki, N., 2018. Novel, diverse RNA viruses from Mediterranean isolates of the phytopathogenic fungus, *Rosellinia necatrix*: insights into evolutionary biology of fungal viruses. Environ. Microbiol. 20, 1464–1483. https://doi.org/10.1111/1462-2920.14065.

Bankevich, A., Nurk, S., Antipov, D., Gurevich, A.A., Dvorkin, M., Kulikov, A.S., Lesin, V. M., Nikolenko, S.I., Pham, S., Prjibelski, A.D., Pyshkin, A.V., Sirotkin, A.V., Vyahhi, N., Tesler, G., Alekseyev, M.A., Pevzner, P.A., 2012. SPAdes: a new genome assembly algorithm and its applications to single-cell sequencing. J. Comput. Biol. 19, 455–477. https://doi.org/10.1089/cmb.2012.0021.

Barnes, I., Crous, P.W., Wingfield, B.D., Wingfield, M.J., 2004. Multigene phylogenies reveal that red band needle blight of Pinus is caused by two distinct species of *Dothistroma, D. septosporum* and *D. pini*. Stud. Mycol. 50, 551–565.

Barnes, I., van der Nest, A., Mullett, M.S., Crous, P.W., Drenkhan, R., Musolin, D.L., Wingfield, M.J., 2016. Neotypification of *Dothistroma septosporum* and epitypification of *D. pini*, causal agents of Dothistroma needle blight of pine. For. Pathol. 46, 388–407. https://doi.org/10.1111/efp.12304.

Bolger, A.M., Lohse, M., Usadel, B., 2014. Trimmomatic: a flexible trimmer for Illumina sequence data. Bioinformatics 30, 2114–2120. https://doi.org/10.1093/bioinformatics/btu170.

Boshra, H., 2022. An Overview of the Infectious Cycle of Bunyaviruses. Viruses. https://doi.org/10.3390/v14102139.

Botella, L., Hantula, J., 2018. Description, distribution, and relevance of viruses of the forest pathogen *Gremmeniella abietina*. Viruses 10, 1–14. https://doi.org/10.3390/v10110654.

Botella, L., Jung, M.H., Rost, M., Jung, T., 2022. Natural populations from the *Phytophthora palustris* complex show a high diversity and abundance of ssRNA and dsRNA viruses. J. Fungi 8, 1118. https://doi.org/10.3390/jof8111118.

Botella, L., Tuomivirta, T.T., Hantula, J., Diez, J.J., Jankovsky, L., 2015a. The European race of *Gremmeniella abietina* hosts a single species of *Gammapartitivirus* showing a global distribution and possible recombinant events in its history. Fungal Biol. 119, 125–135. https://doi.org/10.1016/j.funbio.2014.12.001.

Botella, L., Tuomivirta, T.T., Vervuurt, S., Diez, J.J., Hantula, J., 2012. Occurrence of two different species of mitoviruses in the European race of *Gremmeniella abietina* var. *abietina*, both hosted by the genetically unique Spanish population. Fungal Biol. 116, 872–882. https://doi.org/10.1016/j.funbio.2012.05.004.

Botella, L., Vainio, E.J., Hantula, J., Diez, J.J., Jankovsky, L., 2015b. Description and prevalence of a putative novel mycovirus within the conifer pathogen *Gremmeniella abietina*. Arch. Virol. 160, 1967–1975. https://doi.org/10.1007/s00705-015-2456-5.

Bradshaw, R.E., 2004. Dothistroma (red-band) needle blight of pines and the dothistromin toxin: a review. For. Pathol. 34, 163–185. https://doi.org/10.1111/j.1439-0329.2004.00356.x.

Bruenn, J.A., 1993. A closely related group of RNA-dependent RNA polymerases from double-stranded RNA viruses. Nucleic Acids Res. 21, 5667–5669. https://doi.org/10.1093/nar/21.24.5667.

Buchfink, B., Xie, C., Huson, D.H., 2015. Fast and sensitive protein alignment using DIAMOND. Nat. Methods 12, 59–60. https://doi.org/10.1038/nmeth.3176.

Bulman, L.S., Bradshaw, R.E., Fraser, S., Martín-García, J., Barnes, I., Musolin, D.L., La Porta, N., Woods, A.J., Diez, J.J., Koltay, A., Drenkhan, R., Ahumada, R., Poljakovic-Pajnik, L., Queloz, V., Piškur, B., Doğmuş-Lehtijärvi, H.T., Chira, D., Tomešová-Haataja, V., Georgieva, M., Jankovský, L., Anselmi, N., Markovskaja, S., Papazova-Anakieva, I., Sotirovski, K., Lazarević, J., Adamčíková, K., Boroń, P., Bragança, H., Vettraino, A.M., Selikhovkin, A.V., Bulgakov, T.S., Tubby, K., 2016. A worldwide perspective on the management and control of Dothistroma needle blight. For. Pathol. 46, 472–488. https://doi.org/10.1111/efp.12305.

Bushnell, B., Rood, J., Singer, E., 2017. BBMerge – Accurate paired shotgun read merging via overlap. PLoS ONE 12, e0185056. https://doi.org/10.1371/journal.pone.0185056.

Čermáková, V., Kudláček, T., Rotková, G., Rozsypálek, J., Botella, L., 2017. Hymenoscyphus fraxineus mitovirus 1 naturally disperses through the airborne inoculum of its host, *Hymenoscyphus fraxineus*, in the Czech Republic. Biocontrol Sci. Technol. 27, 992–1008. https://doi.org/10.1080/09583157.2017.1368455.

Chiapello, M., Rodríguez-Romero, J., Ayllón, M.A., Turina, M., 2020. Analysis of the virome associated to grapevine downy mildew lesions reveals new mycovirus lineages. Virus Evol. 6, 1–18. https://doi.org/10.1093/ve/veaa058.

Chiba, Y., Oiki, S., Yaguchi, T., Urayama, S.I., Hagiwara, D., 2021. Discovery of divided RdRp sequences and a hitherto unknown genomic complexity in fungal viruses. Virus Evol. 7, 1–11. https://doi.org/10.1093/ve/veaa101.

Chomczynski, P., Wilfinger, W., Kennedy, A., Rymaszewski, M., Mackey, K., 2010. RNAzol® RT: a new single-step method for isolation of RNA. Nat. Methods 7, 4–5. https://doi.org/10.1038/nmeth.f.315.

Daudu, J., Snowden, J., Tubby, K., Coutts, R., Kotta-Loizou, I., 2019. Studying a mycovirus from *Dothistroma septosporum*, causative agent of pine needle blight. Access Microbiol. 1. https://doi.org/10.1099/acmi.ac2019.po0502.

Dinan, A.M., Lukhovitskaya, N.I., Olendraite, I., Firth, A.E., 2020. A case for a negative-strand coding sequence in a group of positive-sense RNA viruses. Virus Evol. 6, 1–13. https://doi.org/10.1093/ve/veaa007.

Dobin, A., Davis, C.A., Schlesinger, F., Drenkow, J., Zaleski, C., Jha, S., Batut, P., Chaisson, M., Gingeras, T.R., 2013. STAR: ultrafast universal RNA-seq aligner. Bioinformatics 29, 15–21. https://doi.org/10.1093/bioinformatics/bts635.

Drenkhan, R., Tomešová-Haataja, V., Fraser, S., Bradshaw, R.E., Vahalík, P., Mullett, M. S., Martín-García, J., Bulman, L.S., Wingfield, M.J., Kirisits, T., Cech, T.L., Schmitz, S., Baden, R., Tubby, K., Brown, A., Georgieva, M., Woods, A., Ahumada, R., Jankovský, L., Thomsen, I.M., Adamson, K., Marçais, B., Vuorinen, M., Tsopelas, P., Koltay, A., Halasz, A., La Porta, N., Anselmi, N., Kiesnere, R., Markovskaja, S., Kačergius, A., Papazova-Anakieva, I., Risteski, M., Sotirovski, K., Lazarević, J., Solheim, H., Boroń, P., Bragança, H., Chira, D., Musolin, D.L., Selikhovkin, A.V., Bulgakov, T.S., Keča, N., Karadžić, D., Galovic, V., Pap, P., Markovic, M., Poljakovic Pajnik, L., Vasic, V., Ondrušková, E., Piškur, B., Sadiković, D., Diez, J.J., Solla, A., Millberg, H., Stenlid, J., Angst, A., Queloz, V., Lehtijärvi, A., Doğmuş-Lehtijärvi, H.T., Oskay, F., Davydenko, K., Meshkova, V., Craig, D., Woodward, S., Barnes, I., 2016. Global geographic distribution and host range of *Dothistroma species*: a comprehensive review. For. Pathol. 46, 408–442. https://doi.org/10.1111/efp.12290.

Edgar, R.C., 2004. MUSCLE: a multiple sequence alignment method with reduced time and space complexity. BMC Bioinformatics 5, 113. https://doi.org/10.1186/1471-2105-5-113.

EPPO, 2015. PM 7/46 (3) *Lecanosticta acicola* (formerly *Mycosphaerella dearnessii*), *Dothistroma septosporum* (formerly Mycosphaerella pini) and *Dothistroma pini*. EPPO Bull 45, 163–182. https://doi.org/10.1111/epp.12217.

Ferron, F., Weber, F., de la Torre, J.C., Reguera, J., 2017. Transcription and Replication Mechanisms of *Bunyaviridae* and *Arenaviridae* L proteins. Virus Res. https://doi.org/10.1016/j.virusres.2017.01.018.

Forgia, M., Chiapello, M., Daghino, S., Pacifico, D., Crucitti, D., Oliva, D., Ayllon, M., Turina, M., 2022. Three new clades of putative viral RNA-dependent RNA polymerases with rare or unique catalytic triads discovered in libraries of ORFans from powdery mildews and the yeast of oenological interest *Starmerella bacillaris*. Virus Evol. 8, 1–14. https://doi.org/10.1093/ve/veac038.

Gallie, D.R., Walbot, V., 1992. Identification of the motifs within the tobacco mosaic virus 5′-leader responsible for enhancing translation. Nucleic Acids Res. 20, 4631–4638. https://doi.org/10.1093/nar/20.17.4631.

García-Pedrajas, M.D., Cañizares, M.C., Sarmiento-Villamil, J.L., Jacquat, A.G., Dambolena, J.S., 2019. Mycoviruses in biological control: from basic research to field implementation. Phytopathology® 109, 1828–1839. https://doi.org/10.1094/PHYTO-05-19-0166-RVW.

Ghabrial, S.A., Castón, J.R., Jiang, D., Nibert, M.L., Suzuki, N., 2015. 50-plus years of fungal viruses. Virology 356–368. https://doi.org/10.1016/j.virol.2015.02.034, 479–480.

Ghabrial, S.A., Suzuki, N., 2009. Viruses of plant pathogenic fungi. Annu. Rev. Phytopathol. 47, 353–384. https://doi.org/10.1146/annurev-phyto-080508-081932.

Gilbert, K.B., Holcomb, E.E., Allscheid, R.L., Carrington, J.C., 2019. Hiding in plain sight: new virus genomes discovered via a systematic analysis of fungal public transcriptomes. PLoS ONE 14, 1–51. https://doi.org/10.1371/journal.pone.0219207.

Hantula, J., Mäkelä, S., Xu, P., Brusila, V., Nuorteva, H., Kashif, M., Hyder, R., Vainio, E. J., 2020. Multiple virus infections on *Heterobasidion* sp. Fungal Biol. 124, 102–109. https://doi.org/10.1016/j.funbio.2019.12.004.

Heiniger, U., Rigling, D., 1994. Biological control of chestnut blight in Europe. Annu. Rev. Phytopathol. 32, 581–599. https://doi.org/10.1146/annurev.py.32.090194.003053.

Herrero, N., 2017. Identification and sequence determination of a new chrysovirus infecting the entomopathogenic fungus *Isaria javanica*. Arch. Virol. 162, 1113–1117. https://doi.org/10.1007/s00705-016-3194-z.

Hollings, M., 1962. Viruses associated with a die-back disease of cultivated mushroom. Nature 196, 962–965. https://doi.org/10.1038/196962a0.

Hough, B., Steenkamp, E., Wingfield, B., Read, D., 2023. Fungal viruses unveiled: a comprehensive review of mycoviruses. Viruses 15, 1202. https://doi.org/10.3390/v15051202.

Howitt, R.L.J., Beever, R.E., Pearson, M.N., Forster, R.L.S., 2001. Genome characterization of Botrytis virus F, a flexuous rod-shaped mycovirus resembling plant "potex-like" viruses. J. Gen. Virol. 82, 67–78. https://doi.org/10.1099/0022-1317-82-1-67.

Jia, J., Fu, Y., Jiang, D., Mu, F., Cheng, J., Lin, Y., Li, B., Marzano, S.Y.L., Xie, J., 2021. Interannual dynamics, diversity and evolution of the virome in *Sclerotinia sclerotiorum* from a single crop field. Virus Evol. 7, 1–12. https://doi.org/10.1093/ve/veab032.

Jiāng, D., Ayllón, M.A., Marzano, S.Y.L., 2019. ICTV virus taxonomy profile: *Mymonaviridae*. J. Gen. Virol. 100, 1343–1344. https://doi.org/10.1099/JGV.0.001301.

Kashif, M., Jurvansuu, J., Vainio, E.J., Hantula, J., 2019. Alphapartitiviruses of *Heterobasidion* wood decay fungi affect each other's transmission and host growth. Front. Cell. Infect. Microbiol. 9, 1–11. https://doi.org/10.3389/fcimb.2019.00064.

Kim, J.W., Kim, S.Y., Kim, K.M., 2003. Genome organization and expression of the Penicillium stoloniferum virus S. Virus Genes 27, 249–256. https://doi.org/10.1023/A:1026343831909.

Kondo, H., Botella, L., Suzuki, N., 2022. Mycovirus diversity and evolution revealed/inferred from recent studies. Annu. Rev. Phytopathol. 60, 307–336. https://doi.org/10.1146/annurev-phyto-021621-122122.

Kondo, H., Chiba, S., Toyoda, K., Suzuki, N., 2013. Evidence for negative-strand RNA virus infection in fungi. Virology 435, 201–209. https://doi.org/10.1016/j.virol.2012.10.002.

Kopylova, E., Noé, L., Touzet, H., 2012. SortMeRNA: fast and accurate filtering of ribosomal RNAs in metatranscriptomic data. Bioinformatics 28, 3211–3217. https://doi.org/10.1093/bioinformatics/bts611.

Kotta-Loizou, I., Castón, J.R., Coutts, R.H.A., Hillman, B.I., Jiang, D., Kim, D.-H., Moriyama, H., Suzuki, N., 2020. ICTV virus taxonomy profile: Chrysoviridae. J. Gen. Virol. https://doi.org/10.1099/jgv.0.001383.

Leventhal, S.S., Wilson, D., Feldmann, H., Hawman, D.W., 2021. A look into *Bunyavirales* genomes: functions of non-structural (ns) proteins. Viruses. https://doi.org/10.3390/v13020314.

Li, H., Durbin, R., 2009. Fast and accurate short read alignment with Burrows–Wheeler transform. Bioinformatics 25, 1754–1760. https://doi.org/10.1093/bioinformatics/btp324.

Li, H., Handsaker, B., Wysoker, A., Fennell, T., Ruan, J., Homer, N., Marth, G., Abecasis, G., Durbin, R., 2009. The sequence alignment/map format and SAMtools. Bioinformatics 25, 2078–2079. https://doi.org/10.1093/bioinformatics/btp352.

Li, Y., Zhou, M., Yang, Y., Liu, Q., Zhang, Z., Han, C., Wang, Y., 2021. Characterization of the mycovirome from the plant-pathogenic fungus *Cercospora beticola*. Viruses 13. https://doi.org/10.3390/v13101915.

Lin, Y.H., Fujita, M., Chiba, S., Hyodo, K., Andika, I.B., Suzuki, N., Kondo, H., 2019. Two novel fungal negative-strand RNA viruses related to mymonaviruses and phenuiviruses in the shiitake mushroom (*Lentinula edodes*). Virology 533, 125–136. https://doi.org/10.1016/j.virol.2019.05.008.

Linnakoski, R., Sutela, S., Coetzee, M.P.A., Duong, T.A., Pavlov, I.N., Litovka, Y.A., Hantula, J., Wingfield, B.D., Vainio, E.J., 2021. *Armillaria* root rot fungi host single-stranded RNA viruses. Sci. Rep. 11, 7336. https://doi.org/10.1038/s41598-021-86343-7.

Liu, J.J., Chan, D., Xiang, Y., Williams, H., Li, X.R., Sniezko, R.A., Sturrock, R.N., 2016. Characterization of five novel mitoviruses in the white pine blister rust fungus *Cronartium ribicola*. PLoS ONE 11, 1–20. https://doi.org/10.1371/journal.pone.0154267.

Liu, J.J., Xiang, Y., Sniezko, R.A., Schoettle, A.W., Williams, H., Zamany, A., 2019. Characterization of *Cronartium ribicola* dsRNAs reveals novel members of the family *Totiviridae* and viral association with fungal virulence. Virol. J. 16, 1–13. https://doi.org/10.1186/s12985-019-1226-5.

Liu, L., Xie, J., Cheng, J., Fu, Y., Li, G., Yi, X., Jiang, D., 2014. Fungal negative-stranded RNA virus that is related to bornaviruses and nyaviruses. Proc. Natl. Acad. Sci. 111, 12205–12210. https://doi.org/10.1073/pnas.1401786111.

Liu, W., Duns, G., Chen, J., 2008. Genomic characterization of a novel partitivirus infecting *Aspergillus ochraceus*. Virus Genes 37, 322–327. https://doi.org/10.1007/s11262-008-0265-6.

Martínez-Álvarez, P., Vainio, E.J., Botella, L., Hantula, J., Diez, J.J., 2014. Three mitovirus strains infecting a single isolate of *Fusarium circinatum* are the first putative members of the family *Narnaviridae* detected in a fungus of the genus *Fusarium*. Arch. Virol. 159, 2153–2155. https://doi.org/10.1007/s00705-014-2012-8.

Miller, M.A., Pfeiffer, W., Schwartz, T., 2010. Creating the CIPRES Science Gateway for inference of large phylogenetic trees. 2010 Gateway Computing Environments Workshop (GCE). IEEE, pp. 1–8. https://doi.org/10.1109/GCE.2010.5676129.

Morris, T.J., Dodds, J.A., 1979. Isolation and analysis of double-stranded RNA from virus-infected plant and fungal tissue. Phytopathology 69, 854. https://doi.org/10.1094/Phyto-69-854.

Mueller, S., Gausson, V., Vodovar, N., Deddouche, S., Troxler, L., Perot, J., Pfeffer, S., Hoffmann, J.A., Saleh, M.-C., Imler, J.-L., 2010. RNAi-mediated immunity provides

strong protection against the negative-strand RNA vesicular stomatitis virus in *Drosophila*. Proc. Natl. Acad. Sci. 107, 19390–19395. https://doi.org/10.1073/pnas.1014378107.

Mullett, M., Barnes, I., 2012. Dothistroma, in: *Dothistroma* isolation and Molecular Identification Methods. Springer Netherlands, Dordrecht, pp. 176–176.

Mullett, M.S., Adamson, K., Bragança, H., Bulgakov, T.S., Georgieva, M., Henriques, J., Jürisoo, L., Laas, M., Drenkhan, R., 2018. New Country and Regional Records of the Pine Needle Blight Pathogens *Lecanosticta acicola, Dothistroma septosporum* and *Dothistroma pini*. For. Pathol. https://doi.org/10.1111/efp.12440.

Mullett, M.S., Drenkhan, R., Adamson, K., Boroń, P., Lenart-Boroń, A., Barnes, I., Tomšovský, M., Jánošíková, Z., Adamčíková, K., Ondrušková, E., Queloz, V., Piškur, B., Musolin, D.L., Davydenko, K., Georgieva, M., Schmitz, S., Kačergius, A., Ghelardini, L., Orlović, J.K., Müller, M., Oskay, F., Hauptman, T., Halász, A., Markovskaja, S., Solheim, H., Vuorinen, M., Heinzelmann, R., Hamelin, R.C., Konečný, A., 2021. Worldwide genetic structure elucidates the eurasian origin and invasion pathways of *Dothistroma septosporum*, causal agent of Dothistroma needle blight. J. Fungi 7, 1–28. https://doi.org/10.3390/jof7020111.

Muñoz-Adalia, E.J., Diez, J.J., Fernández, M.M., Hantula, J., Vainio, E.J., 2018. Characterization of small RNAs originating from mitoviruses infecting the conifer pathogen *Fusarium circinatum*. Arch. Virol. 163, 1009–1018. https://doi.org/10.1007/s00705-018-3712-2.

Muñoz-Adalia, E.J., Fernández, M.M., Diez, J.J., 2016. The use of mycoviruses in the control of forest diseases. Biocontrol Sci. Technol. 26, 577–604. https://doi.org/10.1080/09583157.2015.1135877.

Nerva, L., Forgia, M., Ciuffo, M., Chitarra, W., Chiapello, M., Vallino, M., Varese, G.C., Turina, M., 2019a. The mycovirome of a fungal collection from the sea cucumber *Holothuria polii*. Virus Res. 273, 197737. https://doi.org/10.1016/j.virusres.2019.197737.

Nerva, L., Turina, M., Zanzotto, A., Gardiman, M., Gaiotti, F., Gambino, G., Chitarra, W., 2019b. Isolation, molecular characterization and virome analysis of culturable wood fungal endophytes in esca symptomatic and asymptomatic grapevine plants. Environ. Microbiol. 21, 2886–2904. https://doi.org/10.1111/1462-2920.14651.

Nibert, M.L., Ghabrial, S.A., Maiss, E., Lesker, T., Vainio, E.J., Jiang, D., Suzuki, N., 2014. Taxonomic reorganization of family *Partitiviridae* and other recent progress in partitivirus research. Virus Res. 188, 128–141. https://doi.org/10.1016/j.virusres.2014.04.007.

Ning, S., Kang, Q., Liu, H., Lu, Y., Sui, L., Xu, W., Shi, W., Li, Q., Zhang, Z., 2022. Interspecific spread of dsRNA mycoviruses in entomogenous fungi *Beauveria* spp. Virus Res. 322, 198933. https://doi.org/10.1016/j.virusres.2022.198933.

O'Brien, C.A., Hobson-Peters, J., Yam, A.W.Y., Colmant, A.M.G., McLean, B.J., Prow, N. A., Watterson, D., Hall-Mendelin, S., Warrilow, D., Ng, M.L., Khromykh, A.A., Hall, R.A., 2015. Viral RNA Intermediates as targets for detection and discovery of novel and emerging mosquito-borne viruses. PLoS Negl. Trop. Dis. 9, 1–27. https://doi.org/10.1371/journal.pntd.0003629.

Okonechnikov, K., Golosova, O., Fursov, M., Team, the U., 2012. Unipro UGENE: a unified bioinformatics toolkit. Bioinformatics 28, 1166–1167. https://doi.org/10.1093/bioinformatics/bts091.

Osaki, H., Sasaki, A., Nomiyama, K., Tomioka, K., 2016. Multiple virus infection in a single strain of *Fusarium poae* shown by deep sequencing. Virus Genes 52, 835–847. https://doi.org/10.1007/s11262-016-1379-x.

Pagnoni, S., Oufensou, S., Balmas, V., Bulgari, D., Gobbi, E., Forgia, M., Migheli, Q., Turina, M., 2023. A collection of *Trichoderma* isolates from natural environments in Sardinia reveals a complex virome that includes negative-sense fungal viruses with unprecedented genome organizations. Virus Evol. 9. https://doi.org/10.1093/ve/vead042.

Park, D., Goh, C.J., Lee, J.S., Sebastiani, F., Hahn, Y., 2020. Identification of Pistacia-associated flexivirus 1, a putative mycovirus of the family *Gammaflexiviridae*, in the mastic tree (*Pistacia lentiscus*) transcriptome. Acta Virol. 64, 28–35. https://doi.org/10.4149/av_2020_104.

Pearson, M.N., Beever, R.E., Boine, B., Arthur, K., 2009. Mycoviruses of filamentous fungi and their relevance to plant pathology. Mol. Plant Pathol. 10, 115–128. https://doi.org/10.1111/j.1364-3703.2008.00503.x.

Preisig, O., Wingfield, B.D., Wingfield, M.J., 1998. Coinfection of a fungal pathogen by two distinct double-stranded RNA viruses. Virology 252, 399–406. https://doi.org/10.1006/viro.1998.9480.

Prospero, S., Botella, L., Santini, A., Robin, C., 2021. Biological control of emerging forest diseases: how can we move from dreams to reality? For. Ecol. Manage. 496, 119377. https://doi.org/10.1016/j.foreco.2021.119377.

Raco, M., Vainio, E.J., Sutela, S., Eichmeier, A., Hakalová, E., Jung, T., Botella, L., 2022. High Diversity of novel viruses in the tree pathogen *Phytophthora castaneae* revealed by high-throughput sequencing of total and small RNA. Front. Microbiol. 13. https://doi.org/10.3389/fmicb.2022.911474.

Ran, H., Liu, L., Li, B., Jiasen, C., Fu, Y., Daohong, J., Xie, J., 2016. Co-infection of a hypovirulent isolate of *Sclerotinia sclerotiorum* with a new botybirnavirus and a strain of a mitovirus. Virol. J. 13, 1–10. https://doi.org/10.1186/s12985-016-0550-2.

Robinson, J.T., Thorvaldsdóttir, H., Winckler, W., Guttman, M., Lander, E.S., Getz, G., Mesirov, J.P., 2011. Integrative genomics viewer. Nat. Biotechnol. 29, 24–26. https://doi.org/10.1038/nbt.1754.

Rombel, I.T., Sykes, K.F., Rayner, S., Johnston, S.A., 2002. ORF-FINDER: a vector for high-throughput gene identification. Gene 282, 33–41. https://doi.org/10.1016/S0378-1119(01)00819-8.

Ruiz-Padilla, A., Rodríguez-Romero, J., Gómez-Cid, I., Pacifico, D., Ayllón, M.A., 2021. Novel mycoviruses discovered in the mycovirome of a necrotrophic fungus. MBio 12. https://doi.org/10.1128/mBio.03705-20.

Rwahnih, M.A., Daubert, S., Úrbez-Torres, J.R., Cordero, F., Rowhani, A., 2011. Deep sequencing evidence from single grapevine plants reveals a virome dominated by mycoviruses. Arch. Virol. 156, 397–403. https://doi.org/10.1007/s00705-010-0869-8.

Sayers, E.W., Bolton, E.E., Brister, J.R., Canese, K., Chan, J., Comeau, D.C., Farrell, C.M., Feldgarden, M., Fine, A.M., Funk, K., Hatcher, E., Kannan, S., Kelly, C., Kim, S., Klimke, W., Landrum, M.J., Lathrop, S., Lu, Z., Madden, T.L., Malheiro, A., Marchler-Bauer, A., Murphy, T.D., Phan, L., Pujar, S., Rangwala, S.H., Schneider, V.A., Tse, T., Wang, J., Ye, J., Trawick, B.W., Pruitt, K.D., Sherry, S.T., 2023. Database resources of the National Center for Biotechnology Information in 2023. Nucleic Acids Res. 51. https://doi.org/10.1093/nar/gkac1032. D29–D38.

Schoebel, C.N., Botella, L., Lygis, V., Rigling, D., 2017. Population genetic analysis of a parasitic mycovirus to infer the invasion history of its fungal host. Mol. Ecol. 26, 2482–2497. https://doi.org/10.1111/mec.14048.

Shah, U.A., Daudu, J.O., Filippou, C., Tubby, K.V., Coutts, R.H.A., Kotta-Loizou, I., 2023. Identification and sequence determination of a new chrysovirus infecting the phytopathogenic fungus *Dothistroma septosporum*. Arch. Virol. 168, 144. https://doi.org/10.1007/s00705-023-05768-9.

Shahi, S., Chiba, S., Kondo, H., Suzuki, N., 2021. Cryphonectria nitschkei chrysovirus 1 with unique molecular features and a very narrow host range. Virology 554, 55–65. https://doi.org/10.1016/j.virol.2020.11.011.

Shamsi, W., Kondo, H., Ulrich, S., Rigling, D., Prospero, S., 2022. Novel RNA viruses from the native range of *Hymenoscyphus fraxineus*, the causal fungal agent of ash dieback. Virus Res. 320, 198901. https://doi.org/10.1016/j.virusres.2022.198901.

Stamatakis, A., Hoover, P., Rougemont, J., 2008. A rapid bootstrap algorithm for the RAxML web servers. Syst. Biol. 57, 758–771. https://doi.org/10.1080/10635150802429642.

Sutela, S., Forgia, M., Vainio, E.J., Chiapello, M., Daghino, S., Vallino, M., Martino, E., Girlanda, M., Perotto, S., Turina, M., 2020. The virome from a collection of endomycorrhizal fungi reveals new viral taxa with unprecedented genome organization. Virus Evol. 6, 1–19. https://doi.org/10.1093/ve/veaa076.

Svanella-Dumas, L., Marais, A., Faure, C., Theil, S., Lefebvre, M., Candresse, T., 2018. Genome characterization of a divergent isolate of the mycovirus Botrytis virus F from a grapevine metagenome. Arch. Virol. 163, 3181–3183. https://doi.org/10.1007/s00705-018-3975-7.

Thapa, V., Roossinck, M.J., 2019. Determinants of coinfection in the mycoviruses. Front. Cell. Infect. Microbiol. https://doi.org/10.3389/fcimb.2019.00169.

Tonka, T., Walterová, L., Hejna, O., Čurn, V., 2022. Molecular characterization of a ssRNA mycovirus isolated from the forest pathogenic fungus *Armillaria ostoyae*. Acta Virol. 66, 290–294. https://doi.org/10.4149/av_2022_309.

Tubby, K., Forster, J., 2021. The potential role of aerial pesticide applications to control landscape-scale outbreaks of pests and diseases in British forestry with a focus on Dothistroma needle blight. For. An Int. J. For. Res. 94, 347–362. https://doi.org/10.1093/forestry/cpaa038.

Tuomivirta, T.T., Hantula, J., 2005. Three unrelated viruses occur in a single isolate of *Gremmeniella abietina* var. *abietina* type A. Virus Res. 110, 31–39. https://doi.org/10.1016/j.virusres.2004.12.005.

Tuomivirta, T.T., Hantula, J., 2003a. *Gremmeniella abietina* mitochondrial RNA virus S1 is phylogenetically related to the members of the genus *Mitovirus*. Arch. Virol. 148, 2429–2436. https://doi.org/10.1007/s00705-003-0195-5.

Tuomivirta, T.T., Hantula, J., 2003b. Two unrelated double-stranded RNA molecule patterns in *Gremmeniella abietina* type A code for putative viruses of the families *Totiviridae* and *Partitiviridae*. Arch. Virol. 148, 2293–2305. https://doi.org/10.1007/s00705-003-0194-6.

Tuomivirta, T.T., Kaitera, J., Hantula, J., 2009. A novel putative virus of *Gremmeniella abietina* type B (*Ascomycota: Helotiaceae*) has a composite genome with endornavirus affinities. J. Gen. Virol. 90, 2299–2305. https://doi.org/10.1099/vir.0.011973-0.

Tuomivirta, T.T., Uotila, A., Hantula, J., 2002. Two independent double-stranded RNA patterns occur in the Finnish *Gremmeniella abietina* var. *abietina* type A. For. Pathol. 32, 197–205. https://doi.org/10.1046/j.1439-0329.2002.00285.x.

Vainio, E.J., 2019. Mitoviruses in the conifer root rot pathogens *Heterobasidion annosum* and *H. parviporum*. Virus Res. 271, 197681. https://doi.org/10.1016/j.virusres.2019.197681.

Vainio, E.J., Chiba, S., Ghabrial, S.A., Maiss, E., Roossinck, M., Sabanadzovic, S., Suzuki, N., Xie, J., Nibert, M., 2018a. ICTV virus taxonomy profile: *Partitiviridae*. J. Gen. Virol. 99, 17–18. https://doi.org/10.1099/jgv.0.000985.

Vainio, E.J., Hantula, J., 2016. Taxonomy, biogeography and importance of *Heterobasidion* viruses. Virus Res. 219, 2–10. https://doi.org/10.1016/j.virusres.2015.10.014.

Vainio, Eeva J., Jurvansuu, J., Hyder, R., Kashif, M., Piri, T., Tuomivirta, T., Poimala, A., Xu, P., Mäkelä, S., Nitisa, D., Hantula, J., 2018b. Heterobasidion partitivirus 13 mediates severe growth debilitation and major alterations in the gene expression of a fungal forest pathogen. J. Virol. 92. https://doi.org/10.1128/JVI.01744-17.

Vainio, E.J., Jurvansuu, J., Streng, J., Rajamäki, M.-L., Hantula, J., Valkonen, J.P.T., 2015a. Diagnosis and discovery of fungal viruses using deep sequencing of small RNAs. J. Gen. Virol. 96, 714–725. https://doi.org/10.1099/jgv.0.000003.

Vainio, E.J., Martínez-Álvarez, P., Bezos, D., Hantula, J., Diez, J.J., 2015b. *Fusarium circinatum* isolates from northern Spain are commonly infected by three distinct mitoviruses. Arch. Virol. 160, 2093–2098. https://doi.org/10.1007/s00705-015-2462-7.

Vainio, E.J., Müller, M.M., Korhonen, K., Piri, T., Hantula, J., 2015c. Viruses accumulate in aging infection centers of a fungal forest pathogen. ISME J. 9, 497–507. https://doi.org/10.1038/ismej.2014.145.

Vainio, E.J., Piri, T., Hantula, J., 2013. Virus community dynamics in the conifer pathogenic fungus *Heterobasidion parviporum* following an artificial introduction of a partitivirus. Microb. Ecol. 65, 28–38. https://doi.org/10.1007/s00248-012-0118-7.

Vainio, E.J., Sutela, S., 2020. Mixed infection by a partitivirus and a negative-sense RNA virus related to mymonaviruses in the polypore fungus *Bondarzewia berkeleyi*. Virus Res. 286, 198079. https://doi.org/10.1016/j.virusres.2020.198079.

van der Nest, A., Wingfield, M.J., Sadiković, D., Mullett, M.S., Marçais, B., Queloz, V., Adamčíková, K., Davydenko, K., Barnes, I., 2023. Population structure and diversity of the needle pathogen *Dothistroma pini* suggests human-mediated movement in Europe. Front. Genet. 14, 1–14. https://doi.org/10.3389/fgene.2023.1103331.

Velasco, L., Arjona-Girona, I., Cretazzo, E., López-Herrera, C., 2019. Viromes in *Xylariaceae* fungi infecting avocado in Spain. Virology 532, 11–21. https://doi.org/10.1016/j.virol.2019.03.021.

Voth, P.D., Mairura, L., Lockhart, B.E., May, G., 2006. Phylogeography of Ustilago maydis virus H1 in the USA and Mexico. J. Gen. Virol. 87, 3433–3441. https://doi.org/10.1099/vir.0.82149-0.

Wang, Q., Li, T., Xu, K., Zhang, W., Wang, X., Quan, J., Jin, W., Zhang, M., Fan, G., Wang, M.-B., Shan, W., 2016. The tRNA-derived small RNAs regulate gene expression through triggering sequence-specific degradation of target transcripts in the oomycete pathogen *Phytophthora sojae*. Front. Plant Sci. 07, 1–14. https://doi.org/10.3389/fpls.2016.01938.

Weber, F., Wagner, V., Rasmussen, S.B., Hartmann, R., Paludan, S.R., 2006. Double-stranded RNA is produced by positive-strand RNA viruses and DNA viruses but not in detectable amounts by negative-strand RNA viruses. J. Virol. 80, 5059–5064. https://doi.org/10.1128/JVI.80.10.5059-5064.2006.

White, T.J., Bruns, T., Lee, S., Taylor, J., 1990. Amplification and direct sequencing of fungal ribosomal RNA genes for phylogenetics. PCR Protocols. Elsevier, pp. 315–322. https://doi.org/10.1016/B978-0-12-372180-8.50042-1.

Wichgers Schreur, P.J., Kormelink, R., Kortekaas, J., 2018. Genome Packaging of the Bunyavirales. Curr. Opin. Virol. https://doi.org/10.1016/j.coviro.2018.08.011.

Zhai, L., Zhang, M., Hong, N., Xiao, F., Fu, M., Xiang, J., Wang, G., Shahi, S., Chiba, S., Kondo, H., Suzuki, N., 2018. Identification and characterization of a novel hepta-segmented dsRNA virus from the phytopathogenic fungus *Colletotrichum fructicola*. Front. Microbiol. 9, 1–13. https://doi.org/10.3389/fmicb.2018.00754.

Zhang, T., Cai, X., Teng, L., Li, X., Zhong, N., Liu, H., 2022. Molecular characterization of three novel mycoviruses in the plant pathogenic fungus *Exobasidium*. Virus Res. 307, 198608. https://doi.org/10.1016/j.virusres.2021.198608.

Zhang, Y.-Z., Chen, Y.-M., Wang, W., Qin, X.-C., Holmes, E.C., 2019. Expanding the RNA virosphere by unbiased metagenomics. Annu. Rev. Virol. 6, 119–139. https://doi.org/10.1146/annurev-virology-092818-015851.